Provisional chapter

Investigation of the Structure and Properties of PVD and PACVD-Coated Magnesium Die Cast Alloys

Tomasz Tański

Additional information is available at the end of the chapter

http://dx.doi.org/10.5772/48165

1. Introduction

The development of existing techniques and technologies depends mainly on the used materials. The applied material determines the manufacturing method for the products. Criteria, which are chose by engineers and technologists for a proper material choice are among others: strength, hardness, elongation, density, corrosion resistance, ability for plastic deformation, or even recycling ability [1-9]. At present engineers have in their disposal modern equipment for investigation of the material structure, which allows it to perform a better and more efficient analysis of the mechanisms responsible for specific properties.

In recent years, there is visible an increasing interest on light metals, and especially materials with low density and relatively high strength properties [1-9]. The group of these materials include particular magnesium and its alloys. Mechanical properties of pure magnesium are relatively low and depends on its purity. In as cast state the tensile strength R_m is in the range of 80 - 120 MPa, yield strength Re = 20 MPa, elongation A = 4 - 6%, and hardness is equal 30 HB. Magnesium is recognised in the periodic table of elements in the group of earth alkali metals and is therefore not to found in nature in the basic form, but only in the form of chemical compounds. As a pure element magnesium has not found wide application possibilities, but as an alloy in combination with other elements such as aluminium, zinc, manganese, silicon, zirconium, thorium, lithium, calcium and rare earth metals, magnesium forms alloys with unique properties, which are used for production of diverse devices and machine- and construction elements. Magnesium alloys are characterised with the lowest density among all non-ferrous metals, as well with a favourable strength to density ratio, which means, that with a lower weight magnesium can hold similar static and dynamic loads compared to aluminium alloys, or even iron alloys. Moreover, these metals have a high vibration damping capacity and good casting properties, similar to these of aluminium cast alloys.

Magnesium alloys are used for production of different types of car accessories such as steering wheels, pedals, wheels, seat frames, inlet manifolds, gear housings and other elements (Table 1) [1-9].

Stability of raw material cost and supply	the abundance of natural resources together with the cost effective primary processes contribute to a stable supply that can rapidly grow to meet future demand
Lower weight	magnesium is the lightest structural metal. It is lighter than aluminum by 35 percent and lighter than zinc by 73 percent. Its excellent strength-to-weight ratio significantly decreases the weight and cost of magnesium components
Durability	magnesium is a durable metal with excellent capacity for damping vibrations
Machinability	magnesium is the easiest metal to machine, which leads to rapid processing and the cost effective production of finished parts
Perfect for complex applications	in the die casting process magnesium can be formed into very complicated and thin-walled parts with a high degree of precision
Shielding against electromagnetic radiation	magnesium alloys, due to their excellent conductivity, shield against harmful electromagnetic radiation and are an ideal material to be used in electronic equipment, where electromagnetic radiation is an issue
Market growth	the increase in the use of magnesium applications is approximately 15-20 percent annually

Table 1. Magnesium alloys properties [1,2,8]

Increasingly, they find their application in the sports industry. They are also used for production of bicycle frames, ski and other sports equipment, etc. Beside the automotive and sport industry these alloys are used for construction elements, machinery and equipment, industrial automation, electronics, also in the military industry, and in the electrical branches (Table 1). Magnesium alloys are recognized as materials with high potential application possibilities, what is increasingly reflected in its increasing popularity and usage in production. Thanks to innovatory technologies, it is possible to perform castings from a few grams to several kilograms in weight. These alloys due to the number of its benefits will soon become an indispensable standard in the automotive, sports and aviation industry [1-9]. The growing trends in the production of magnesium alloys point at the increased necessity of their application in the world constructional industry, and the magnesium alloys will become one of the most frequent materials used in the following decades.

Optimization of chemical composition and technological conditions, production, casting and heat treatment of light metal alloys, due to the excellent set of mechanical properties and corrosion resistance based on the analysed precipitation- and phase transitions processes occurring in the investigated alloys during their cooling process is just one of the existing possibilities applicable for the enhancement of mechanical properties. Taking into account, that some properties are of interest only for the surface of the material, investigations were carried out concerning surface treatment of the magnesium alloys by applying of the physical vapour deposition processes. Due to insufficient stiffness of the substrate material a dual coating system was applied with a variable coating hardness, consisting of a soft ground - transition gradient layer - and a hard, wear-resistant outer layer. Thin hard PVD coatings on a soft surface, seams to be a preferred combination from the tribological point of view. Such coatings have found its special application for components working tribo-corrosive environment [10-16].

The aim of this research work is to determine the nature and properties of two-layer coating in a gradient like and hard wear resistant layer configuration, produced using the PVD and PACVD process on magnesium alloy substrate. Taking into account the optimisation of chemical composition and the development of optimal production conditions for achieving highest possible mechanical properties, corrosion resistance and functional properties compared to the existing standard surface layers.

2. Experimental procedure

The investigations have been carried out on test pieces of MCMgAl12Zn1 (Table 2, No. 1), MCMgAl9Zn (Table 2, No.2), MCMgAl6Zn (Table 2, No. 3), MCMgAl3Zn1 (Table 2, No. 4) magnesium alloys in as-cast and after heat treatment states. The chemical composition of the investigated materials is given in Table 2.

The mass concentration of main elements, %							
No.	Al	Zn	Mn	Si	Fe	Mg	Rest
1	12.1	0.62	0.17	0.047	0.013	86.96	0.0985
2	9.09	0.77	0.21	0.037	0.011	89.79	0.0915
3	5.92	0.49	0.15	0.037	0.007	93.33	0.0613
4	2.96	0.23	0.09	0.029	0.006	96.65	0.0361

Table 2. Chemical composition of investigated alloys, %

The coating deposition process of the coatings: Ti/TiCN/TiAlN and Cr/CrN/CrN was made in a device based on the cathodic arc evaporation method in an Ar, N_2 and C_2H_2 atmosphere moreover the DLC coating were deposited using acetylene (C_2H_2) as precursor and was produced by PACVD process (Table 3). Cathodes containing pure metals (Cr, Ti) and the TiAl

(50:50 at. %) were used for deposition of the coatings. The diameter of the used cathodes was 65 mm. After pumping the chamber the base pressure was 5x10-3 Pa (Table 3).

The temperature was controlled by thermocouples. Then the substrates were cleaned by argon ion at the pressure 2 Pa for 20 min. To improve the adhesion of coatings, a transition Cr or Ti interlayer was deposited. The working pressure during the deposition process was 2-4 Pa depending of the coatings type. The distance between each of the cathodes and the deposited substrates was 120 mm.

The examinations of thin foils microstructure and phase identification were made on the JEOL 3010CX transmission electron microscope (TEM), at the accelerating voltage of 300 kV using selected area diffraction method (SAD) for phase investigations. The diffraction patterns from the TEM were solved using a special computer program "Eldyf" software supplied by the Institute of Material Science o the University of Silesia. TEM specimens were prepared by cutting thin plates from the material. The specimens were ground down to foils with a maximum thickness of 80 μm before 3 mm diameter discs were punched from the specimens. The disks were further thinned by ion milling method with the Precision Ion Polishing System (PIPS™), used the ion milling device model 691 supplied by Gatan until one or more holes appeared. The ion milling was done with argon ions, accelerated by a voltage of 15 kV, energy and angle are presented in Table 4.

Process parameters	Coating type		
	Ti/TiCN-gradient/ TiAlN	Cr/CrN-gradient/CrN	Ti/DLC/DLC
Base pressure [Pa]	510^{-3}	510^{-3}	$1x10^{-3}$
Working pressure [Pa]	9.010-1/1.1÷1.9/2.8	1.0/1.4÷2.3/2.2	2
Argon flow rate measurement [sccm]	80*	80*	80*
	10**	80**	-
	10***	20***	-
Nitrogen flow rate measurement [sccm]	0225**	0250**	-
	350***	250***	-
Acetylene flow rate measurement [sccm]	1400**	-	230
Substrate bias voltage [V]	70*	60*	500
	70**	60**	
	70***	60***	
Target current [A]	60	60	-
Process temperature [ºC]	<150	<150	<180

Table 3. Deposition parameters of the investigated coatings*during metallic layers deposition, **during gradient layers deposition, *** during ceramic layers deposition

Angle [°]	Energy [KeV]	Time [min]
6	3.8	180
3	3.2	15

Table 4. Ion milling parameters using for polishing

Microstructure investigation was performed using scanning electron microscope (SEM) ZEISS Supra 25 with a magnification between 10000 and 35000 times. For microstructure evaluation the Secondary Electrons (SE) detection was used, with the accelerating voltage of 5÷25 KV. For a complex metallographic analysis of the fractures of the investigated samples, the material with the coated layer was initially cut, and before braking cooled down in liquid nitrogen. Qualitative and quantitative chemical composition analysis in micro-areas of the investigated coatings was performed using the X-Ray microanalysis (EDS) by mind of the spectrometer EDS LINK ISIS supplied by Oxrord. This device is attached to the electron scanning microscope Zeiss Supra 35. The investigations were performed by an accelerating voltage of 20 kV.

The analysis of phase composition of the substrates and of the obtained coatings was carried out using the X-ray diffraction method (XRD) on the X-ray apparatus X'Pert of the Panalytical Company using the filtered radiation of a cobalt lamp. For the reason of put on diffraction pattern coming from the substrate material and coating ones as well as their intensity, and also convergence of the Miller indexes for different coating types to achieve a more accurate information from the surface layer and decrease of the substrate influence on the diffraction pattern in the future investigations a diffraction technique was applied with a constant angle of incidence of the primary X-Ray beam using parallel beam collimator placed before the proportional detector. Diffraction pattern of gradient- and multilayer coatings were achieved by different angle of incidence of the primary beam. The effective depth of measurement was chosen experimentally on the basis of preliminary investigations of different angles of incidence.

The specimens were tested on Raman spectroscope from Renishaw, type inVia Raman Microscope, coupled with light microscope; for observation has been used laser with wavelength 514nm and full power equal to 30mW; after precise alignment of the laser spot the data was obtained in single spectral acquisition with use of 20x long working distance plan objective lens.

The cross-sectional atomic composition of the samples (coating and substrate) was obtained by using a glow discharge optical spectrometer, GDOS-750 QDP from Leco Instruments. The following operation conditions of the spectrometer Grimm lamp were fixed during the tests:

- lamp inner diameter – 4 mm;

- lamp supply voltage – 700 V;
- lamp current – 20 mA;
- working pressure – 100 Pa.

Wear resistance investigations were performed using the ball-on-disk method in dry friction conditions in horizontal settlement of the rotation axis of the disk. As the counterpart there was used a tungsten carbide ball with a diameter of 3 mm. The tests were performed at room temperature by a defined time using the following test conditions:

- load, Fn-5N,
- rotation of the disk 200 turns/min,
- wear radius of 2.5 mm,
- shift rate of -0, 05 m/s.

The measurement of roughness of the surface of the obtained coatings was carried out using the profilographometer Diavite Compact of Asmeo Ag Company. The measurement length of Lc=0.8 mm and measurement accuracy of ±0.02 μm. The parameter Ra acc. the Standard PN-EN ISO 4287:1999 was assumed as the quantity describing the roughness. On each investigated sample there was performed 6 measurements and we determined the average.

3. Results and discussions

Results of diffraction method investigations achieved by the high resolution transmission electron microscope allow to identify the TiAlN, CrN, graphit phase occurred in the surface layer (Fig. 1-12). For all investigated alloys a nanocrystalline microstructure of the surface layer in investigated area was detected. On figure 1, 2, there are showed the microstructures of the layer TiAlN phase, using the dark field technique the size of the subgrains or crystallites can be determined, as ca. 15 nm in diameter. For phase determination of the structure of the surface layer diffraction pattern analysis of the investigated areas has allow it to identify the (Ti,Al)N phase as a cubic phase of the 225-Fm3m space group with the d-spacing of a=b=c=0,424173 nm. The CrN phase was determined as a cubic phase of the 225-Fm3m space group with the d-spacing of a=b=c=0.414 nm. Investigations performed using particularly the dark field technique on the transmission electron microscope have confirmed that the size of the CrN crystallites, in the majority of the cases does not exceed the limit of ~ 20 nm (Fig. 5,6). Also a globular bulk shaped morphology and homogeneity of these crystallites was found, as well a low statistical dispersion in the range between 10 to 20 nm.

http://dx.doi.org/10.5772/48165

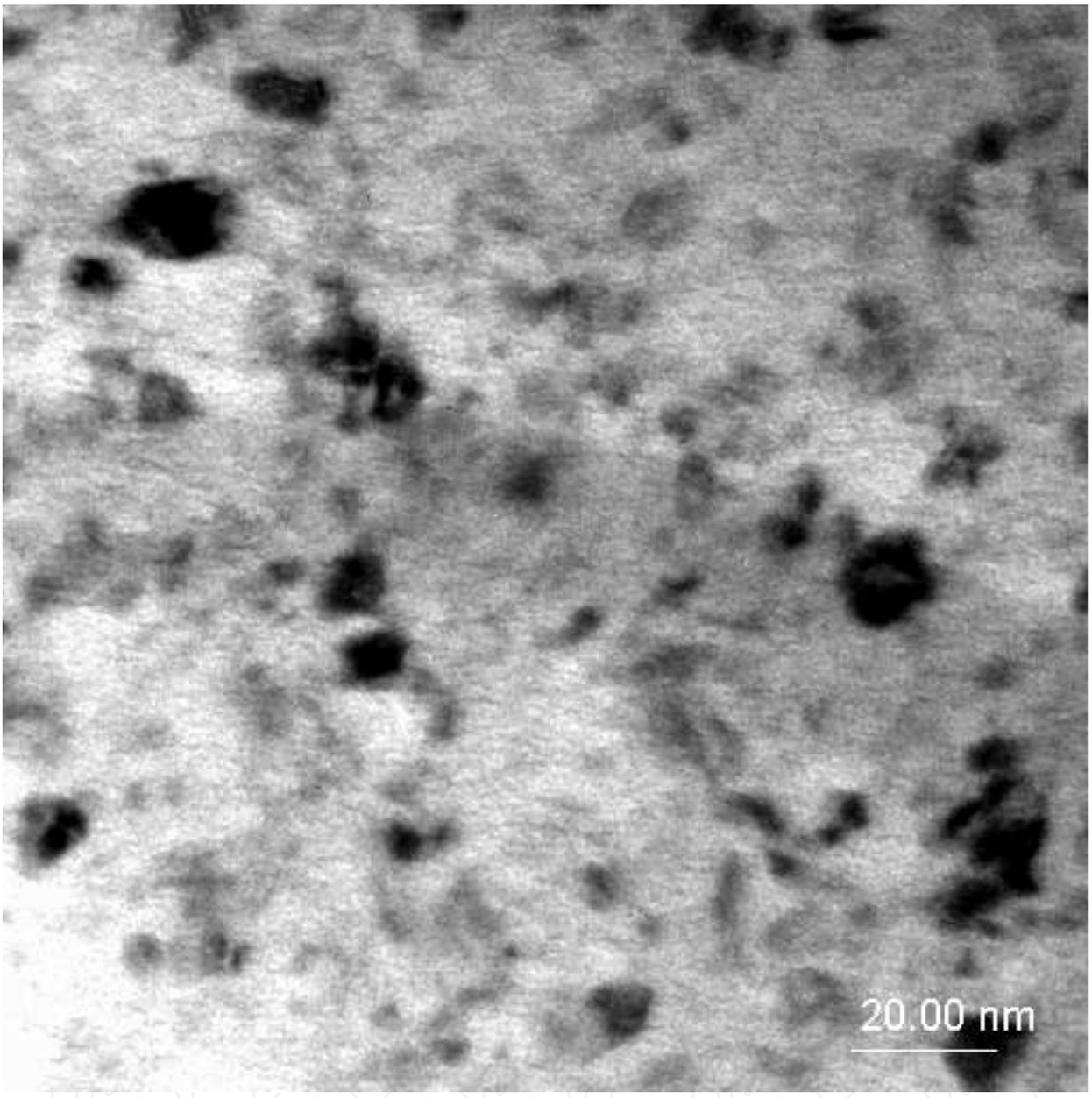

Figure 1. Structure of the thin foil from TiAlN surface layer (Ti/TiCN/TiAlN coating), bright field, TEM

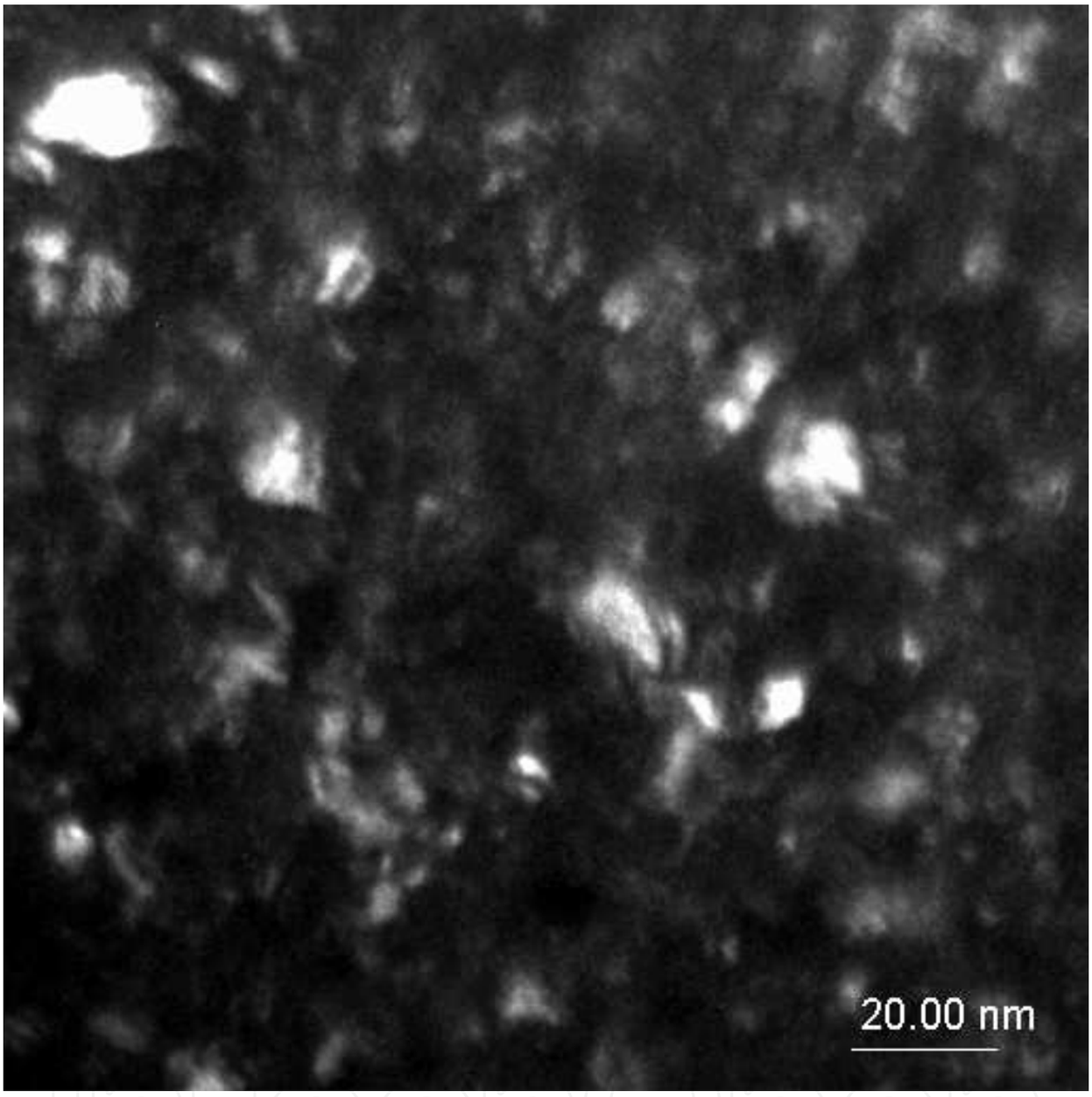

Figure 2. Structure of the thin foil from TiAlN surface layer (Ti/TiCN/TiAlN coating), dark field, TEM

http://dx.doi.org/10.5772/48165

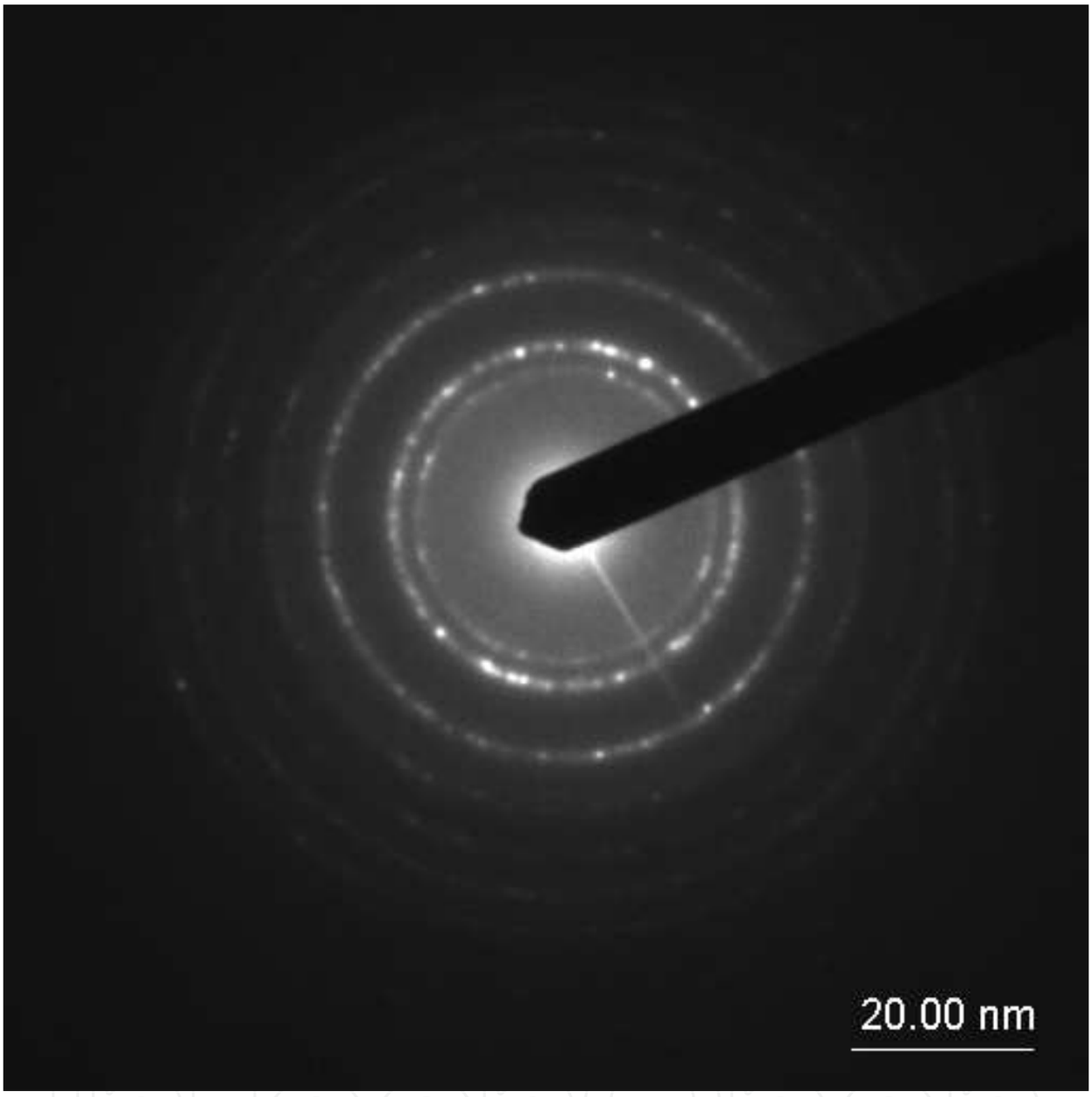

Figure 3. Diffraction pattern of the thin foil from TiAlN surface layer (Ti/TiCN/TiAlN coating) presented on Fig. 1

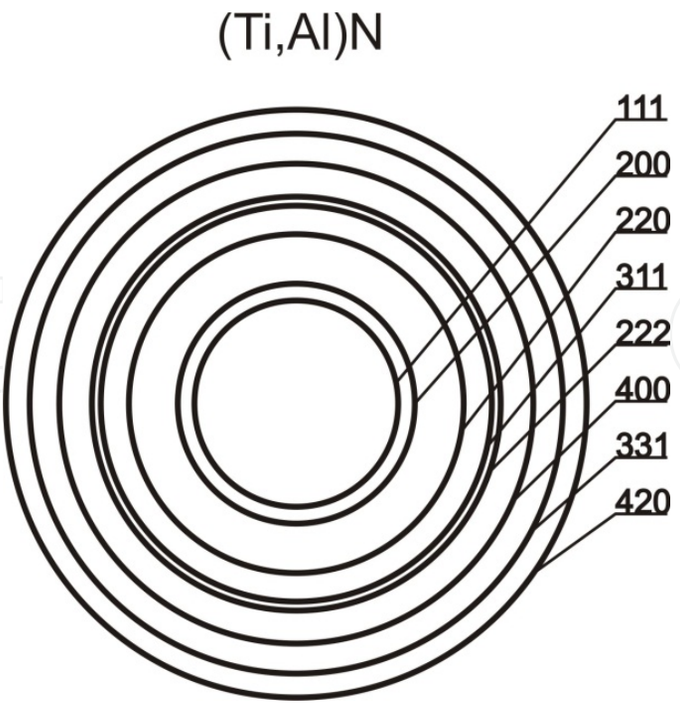

Figure 4. Solution of the diffraction pattern presented on Fig. 3 for the (Ti, Al)N phase

http://dx.doi.org/10.5772/48165

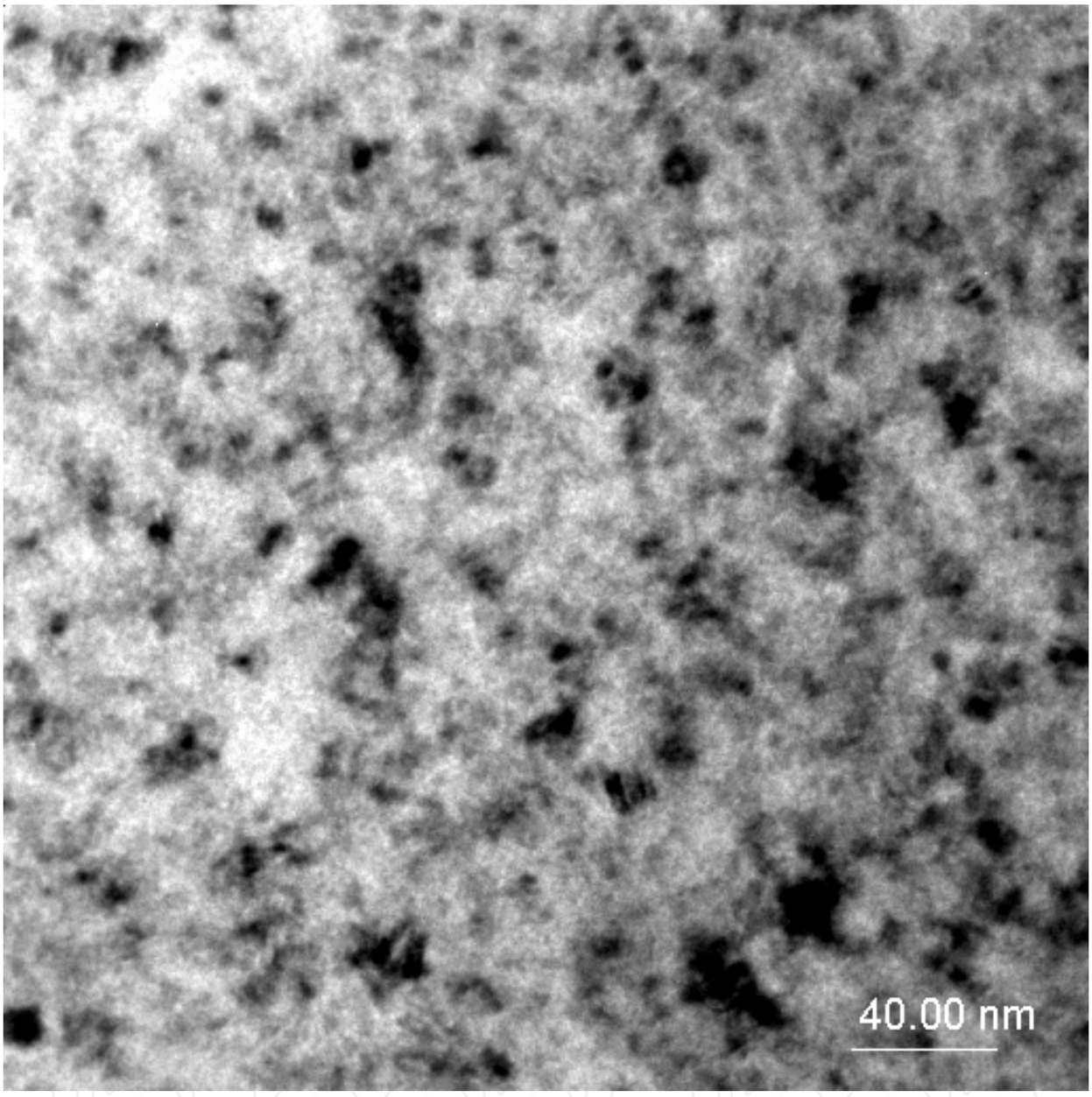

Figure 5. Structure of the thin foil from CrN surface layer (Cr/CrN/CrN coating), bright field, TEM

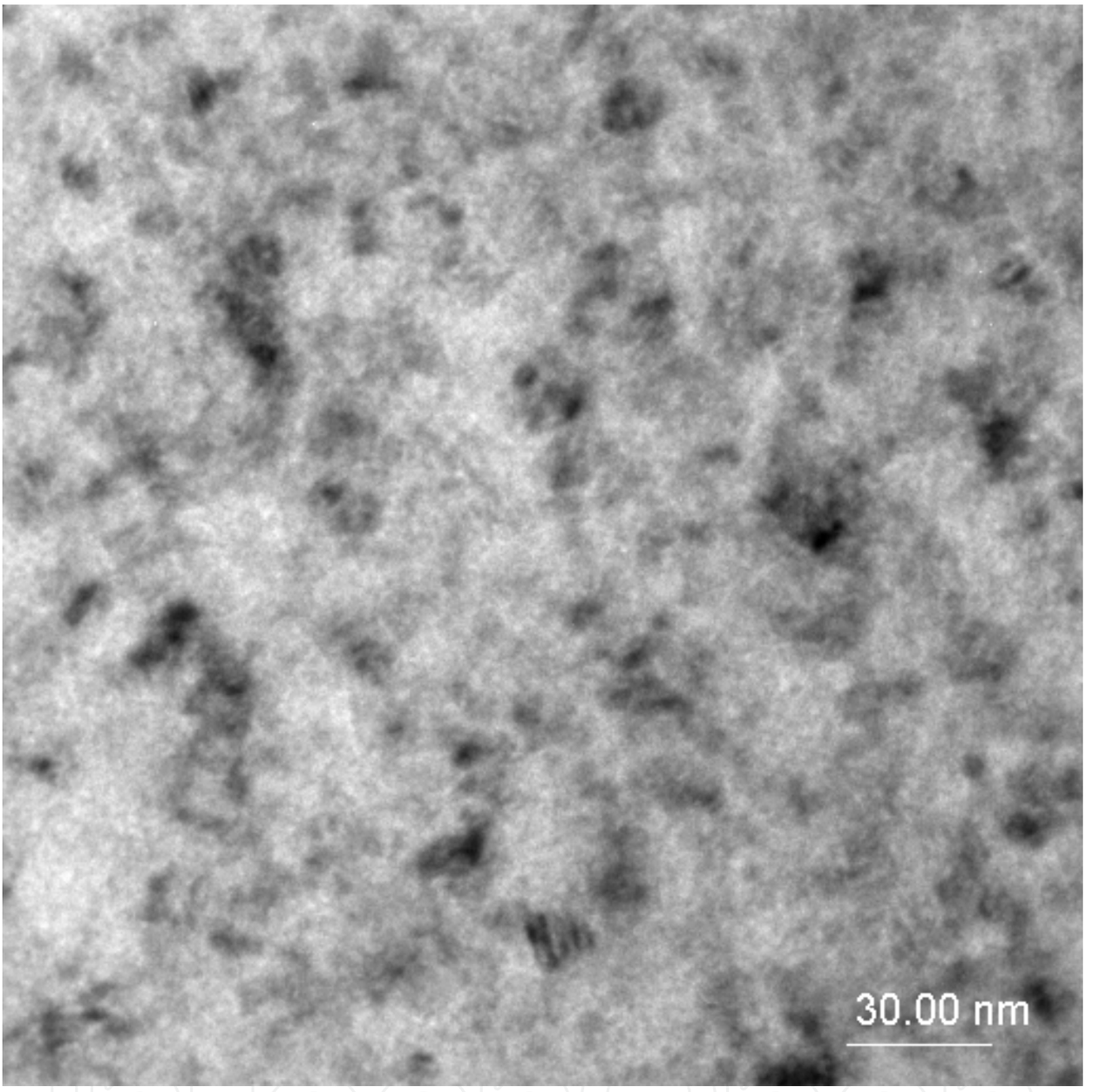

Figure 6. Structure of the thin foil from CrN surface layer (Cr/CrN/CrN coating), bright field, TEM

http://dx.doi.org/10.5772/48165

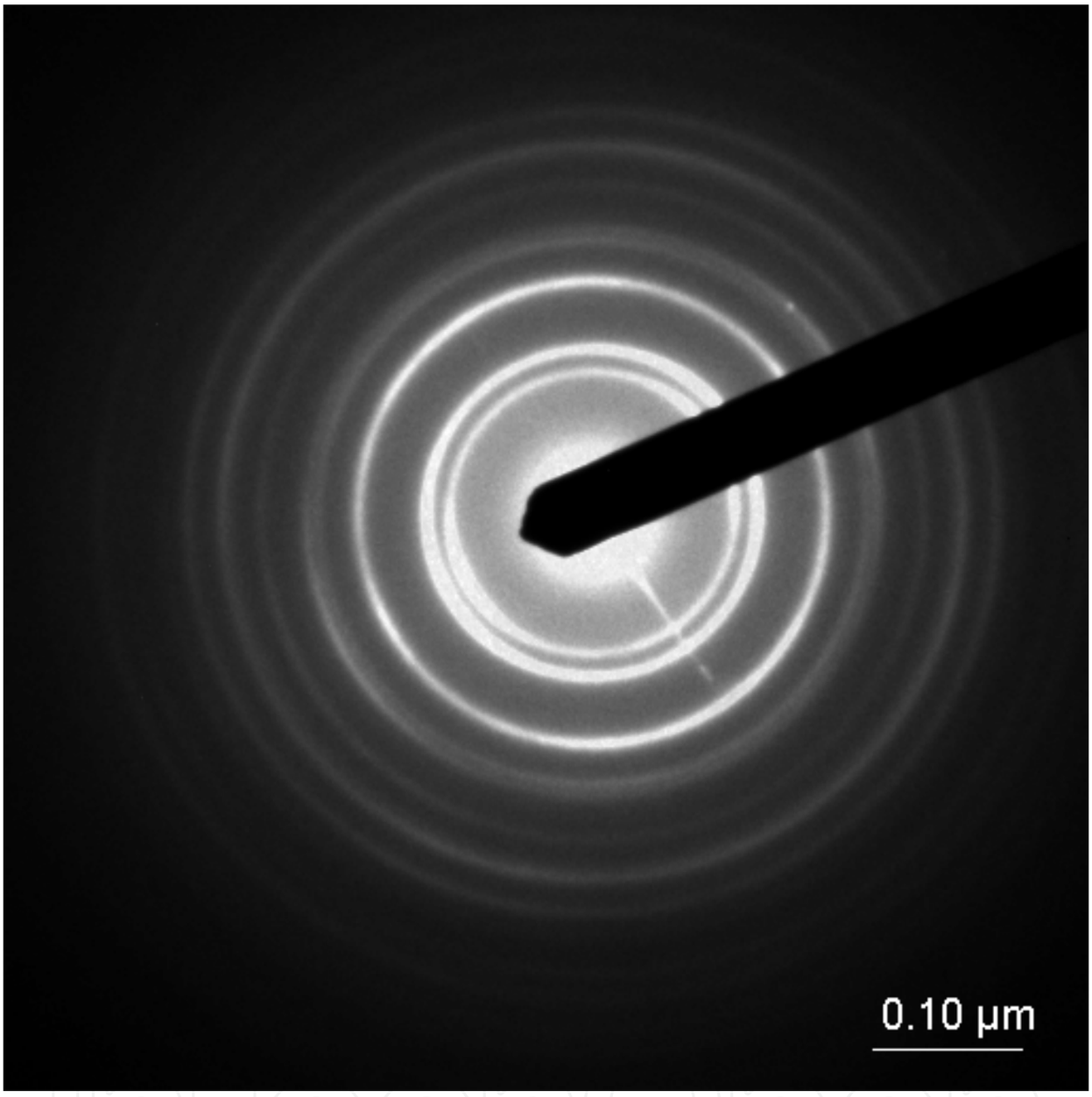

Figure 7. Diffraction pattern of the thin foil from CrN surface layer (Cr/CrN/CrN coating) presented on Fig. 5

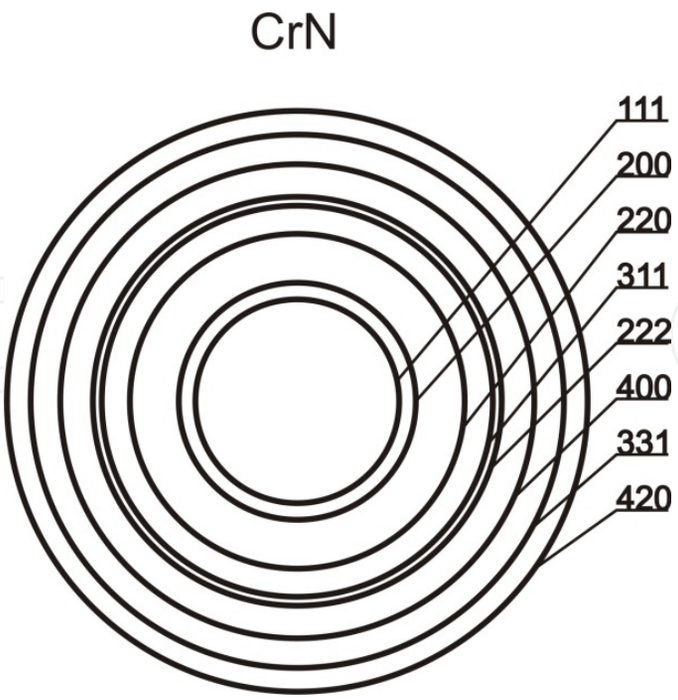

Figure 8. Solution of the diffraction pattern presented on Fig. 7 for the CrN phase

The graphite phase was determined as a hexagonal phase of the 186-P63mc space group with the lattice parameters of a=b=0.2, c=0.679 nm (Fig. 9,10). Investigations performed using particularly the dark field technique on the transmission electron microscope have confirmed, that the size of the graphite crystallites, which the Ti/DLC/DLC coating is constant, is in the range up to 30 nm and with irregular shape.

Investigations of the fractures of the magnesium alloys coated with the Ti/TiCN/TiAlN, Cr/CrN/CrN, Ti/DLC/DLC layers show an occurrence of sharp transition zone between the substrate and coating (Fig. 13-18). It was found out, as a result of the microstructure investigations on scanning electron microscope, that there are no pores or cracks in the produced coating and no defects and failures occurring spontaneously in this single layer are of significant importance for the properties of the whole layer (Fig. 13-18). The thickness of the Ti/TiCN/TiAlN layer is in the range up to 3.3 μm, Cr/CrN/CrN layer is in the range up to 1.9 μm, and Ti/DLC/DLC layer is in the range up to 2,5 microns.

In the case of the Ti/TiCN/TiAlN layer it was also found that the examined layers were not uniform and consisted of three sub-layers, with a clearly visible transition zone between the gradient layer and the wear resistant coating achieved using separate metals evaporation sources, where the upper one had a thickness of ca. 0.6 μm (Fig. 13, 14). Coating thickness was measured using a scanning electron microscope. Fracture morphology of the investigated coatings is characterised by a lack of columnar structure (Fig. 13-18). On the basis of the performed observations on scanning electron microscope the coating of the Ti/TiCN/TiAlN type show an increasing non-homogeneity compared to the Cr/CrN/CrN and Ti/DLC/DLC coatings what is connected with the presence of numerous droplet-shaped microparticles

http://dx.doi.org/10.5772/48165

(their number depends on the type of the target) and should that fore significantly influence mechanical properties and resistance of the investigated surfaces (Fig. 13-20). The droplets observed in SEM are noticeably different in terms of size and shape (regular and irregular shape, slightly flat). There were also some hollows formed probably when the solidified droplets break off after the used process has been completed (Fig. 19,20).

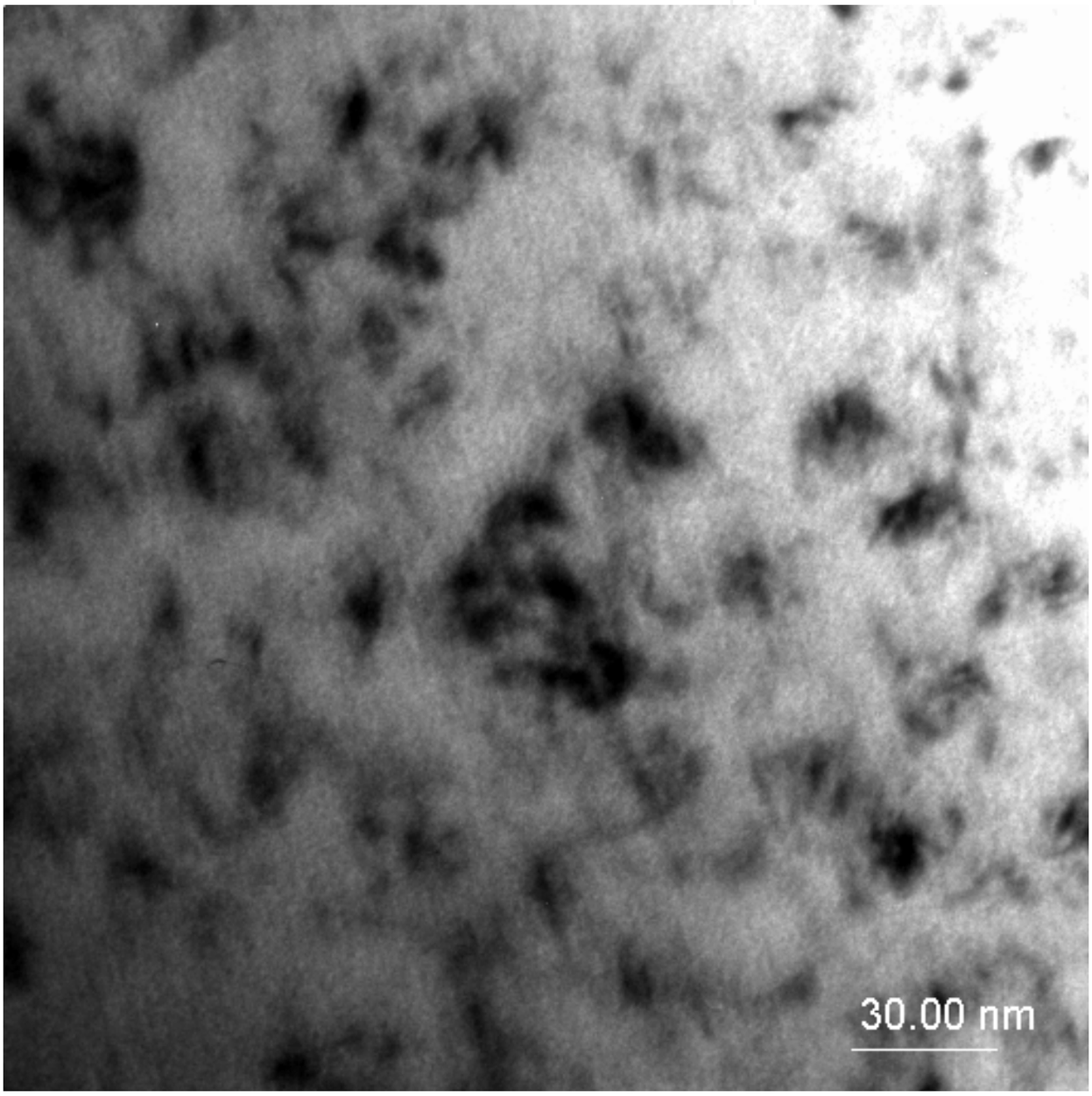

Figure 9. Structure of the thin foil from DLC surface layer (Ti/DLC/DLC coating), bright field, TEM

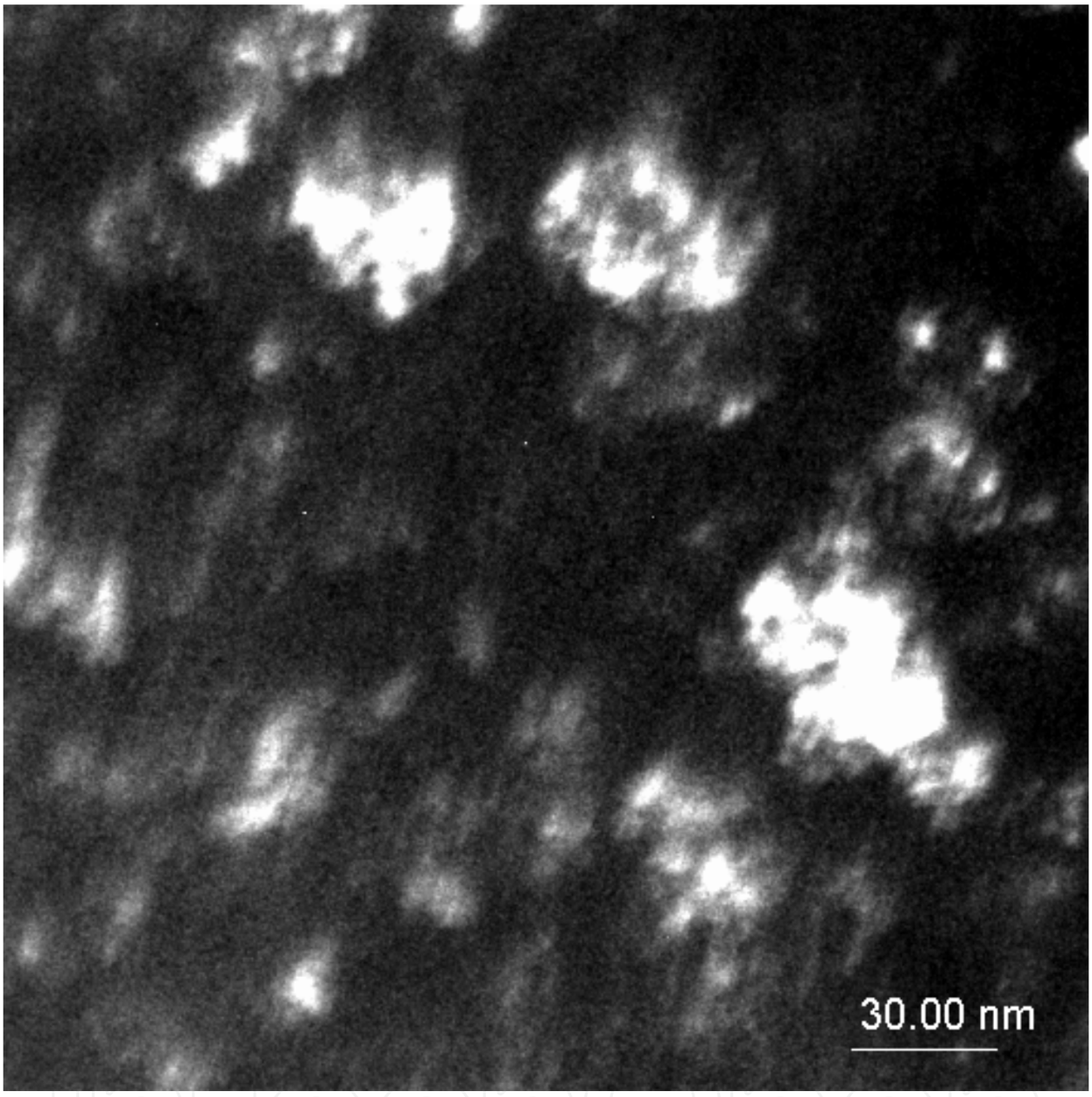

Figure 10. Structure of the thin foil from DLC surface layer (Ti/DLC/DLC coating), dark field, TEM

http://dx.doi.org/10.5772/48165

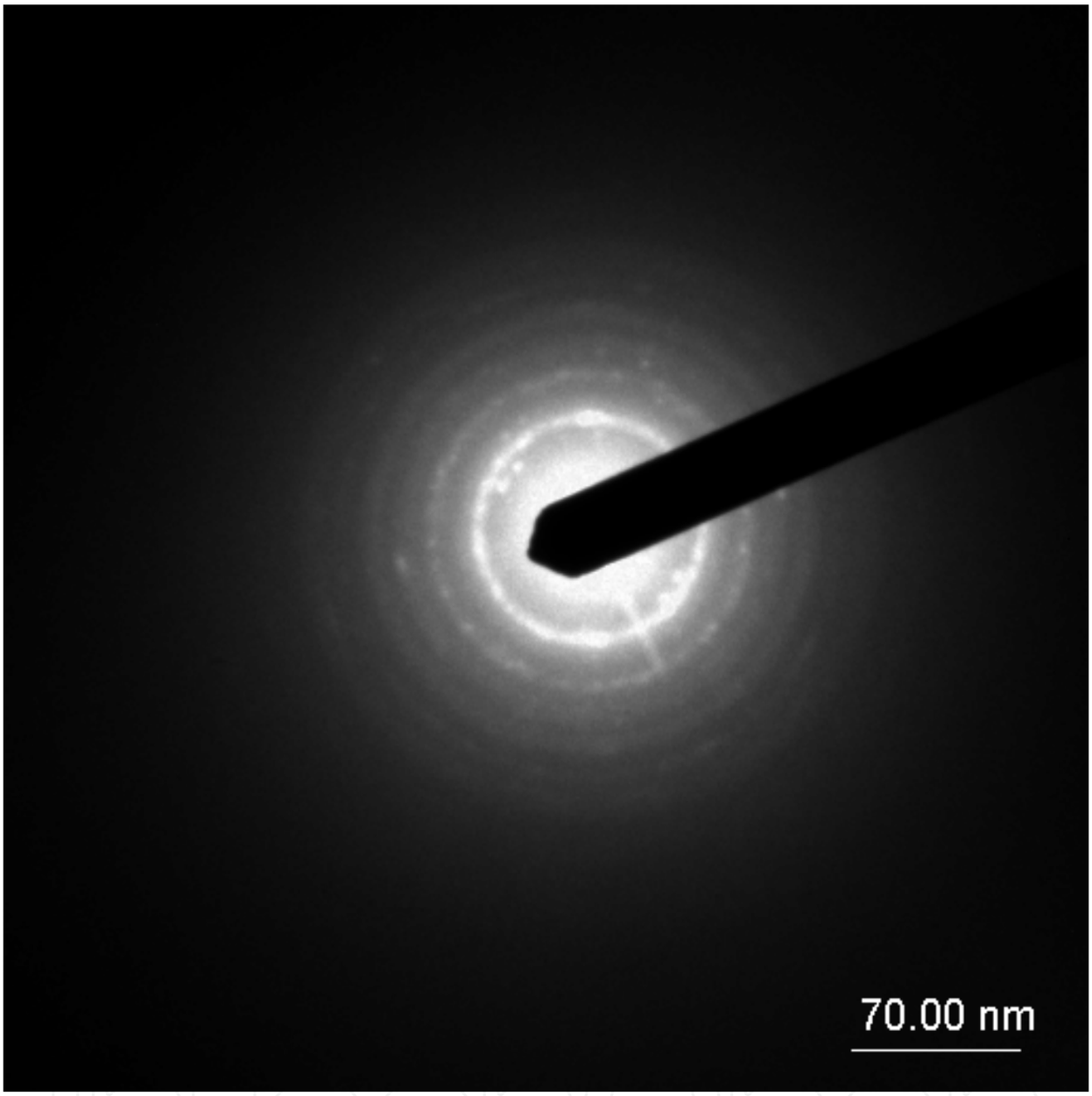

Figure 11. Diffraction pattern of the thin foil from DLC surface layer (Ti/DLC/DLC coating) presented on Fig. 9

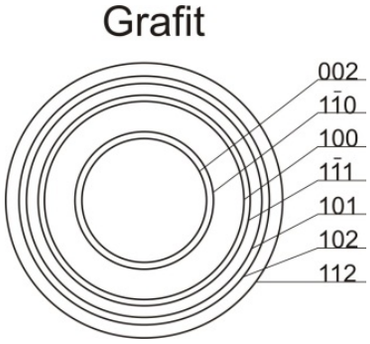

Figure 12. Solution of the diffraction pattern presented on Fig. 11 for the graphite phase

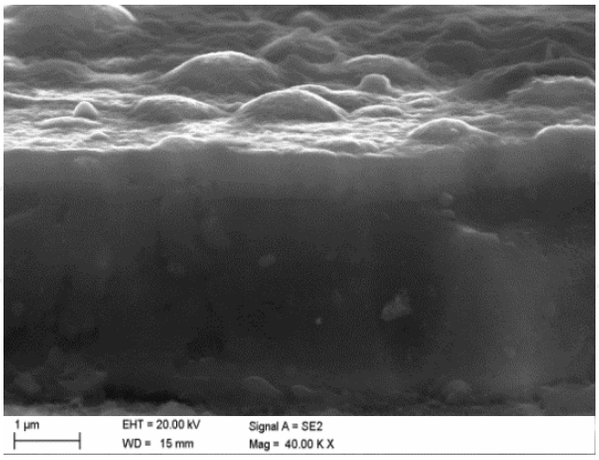

Figure 13. Cross-section SEM images of the Ti/TiCN/TiAlN coating deposited onto the AZ91 substrate

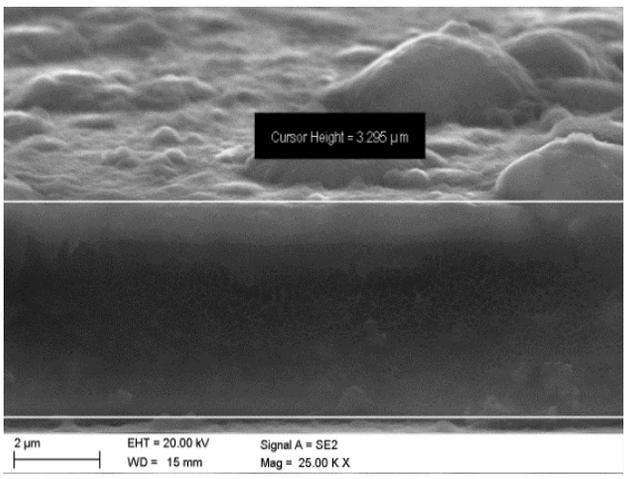

Figure 14. Cross-section SEM images of the Ti/TiCN/TiAlN coating deposited onto the AZ91 substrate

http://dx.doi.org/10.5772/48165

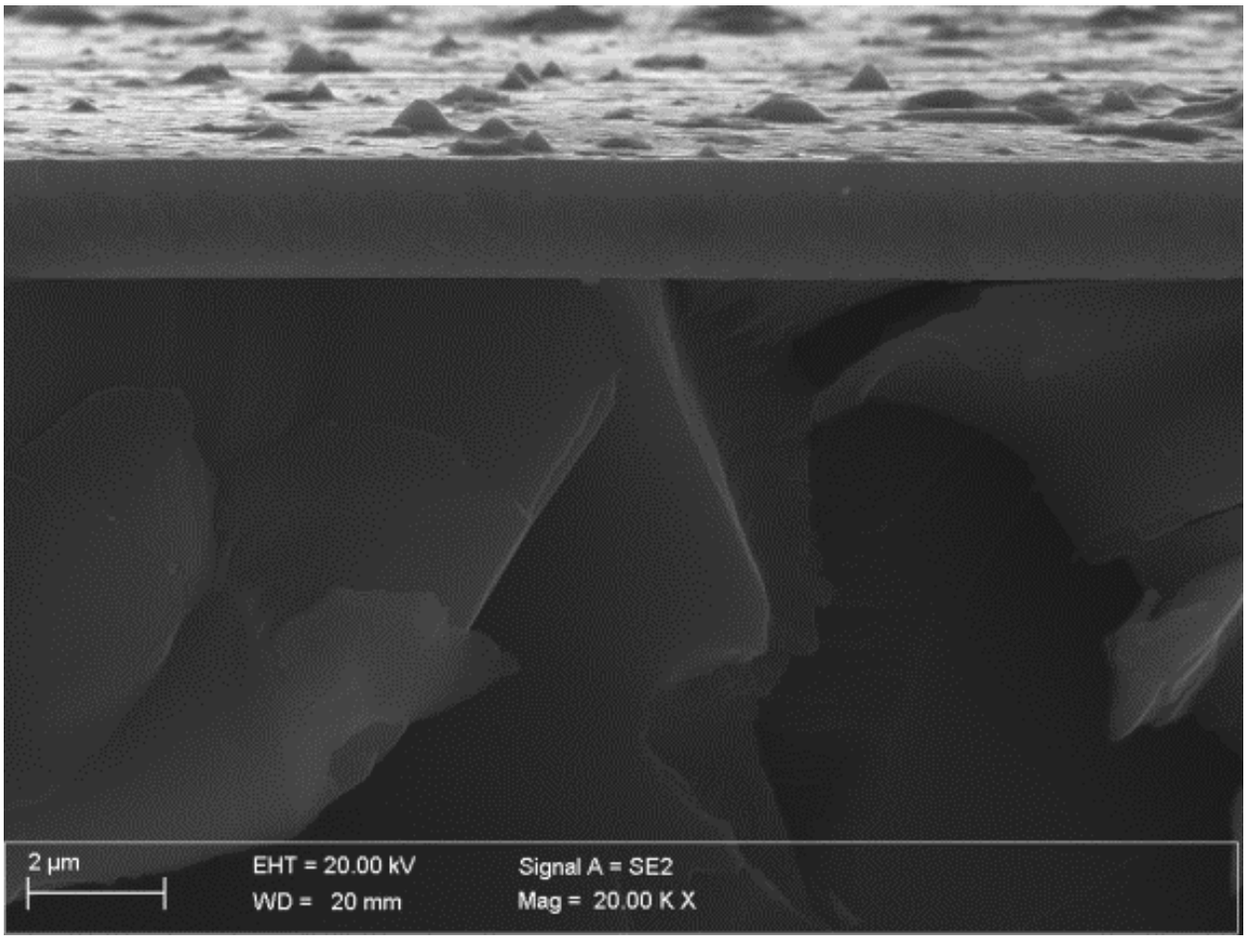

Figure 15. Cross-section SEM images of the Cr/CrN/CrN coating deposited onto the AZ121 substrate

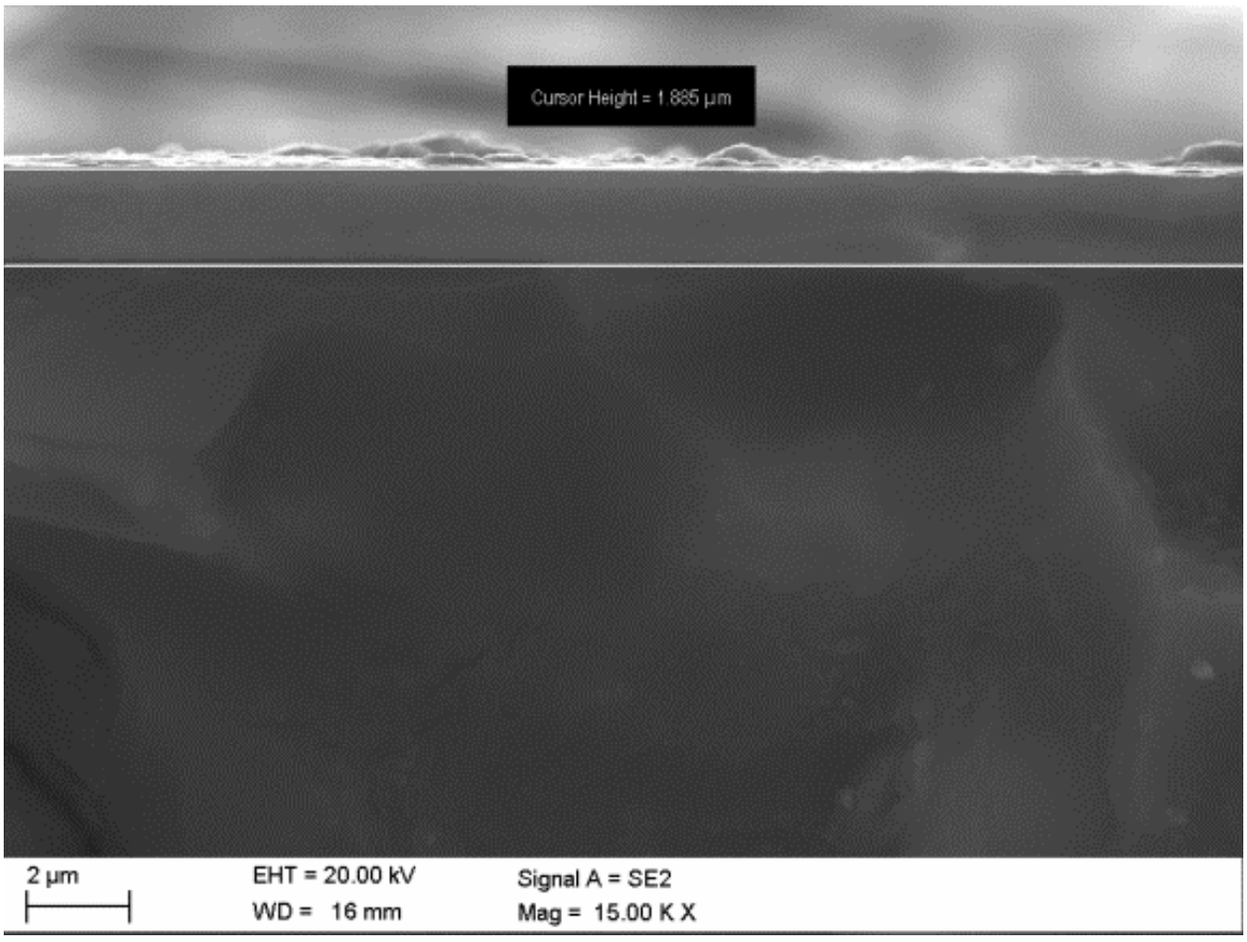

Figure 16. Cross-section SEM images of the Cr/CrN/CrN coating deposited onto the AZ61 substrate

As a result of the performed X-ray microanalysis using the qualitative energy spectrometer EDS it was confirmed the presence of major alloying elements Mg, Al, Zn, N, Cr, as compounds of the investigated alloys as well of the coatings (in this case Cr/CrN/CrN coating) (Fig. 21). Moreover qualitative analysis of the chemical elements distribution performed on the cross-section of the investigated sample clearly confirms increase of the concentration of the elements at grain boundaries of the produced coatings (Fig. 21).

http://dx.doi.org/10.5772/48165

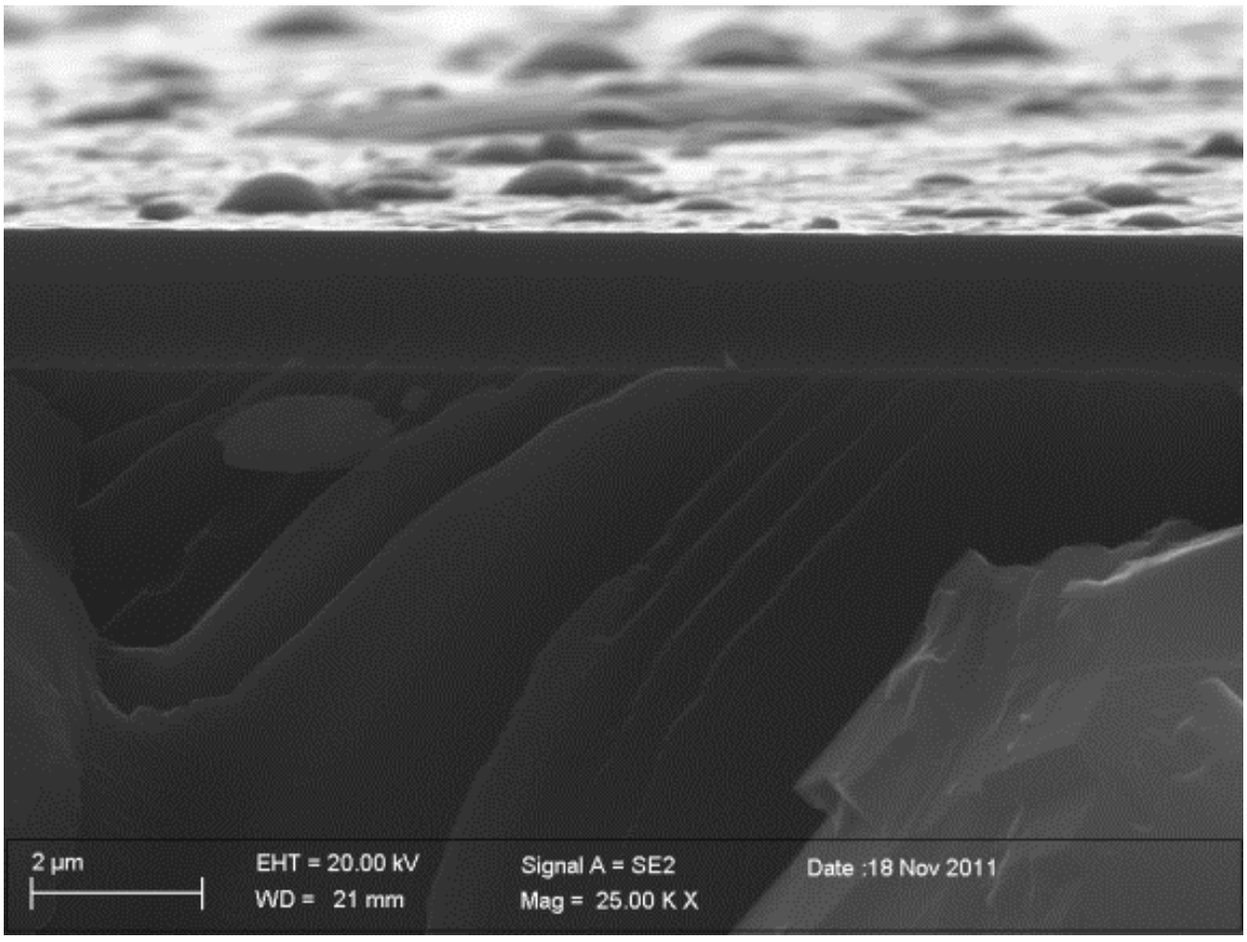

Figure 17. Cross-section SEM images of the Ti/DLC/DLC coating deposited onto the AZ121 substrate

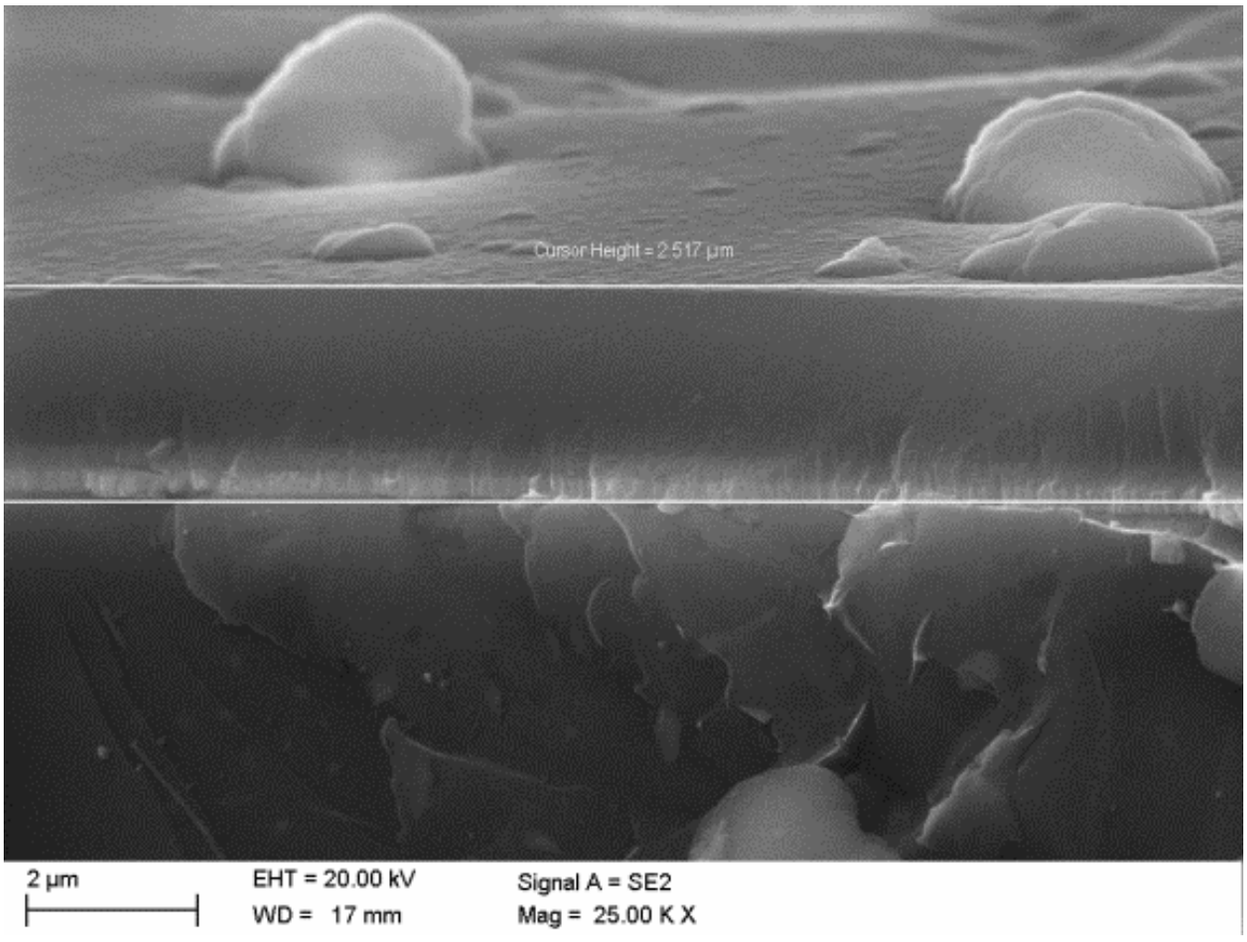

Figure 18. Cross-section SEM images of the Ti/DLC/DLC coating deposited onto the AZ61 substrate

http://dx.doi.org/10.5772/48165

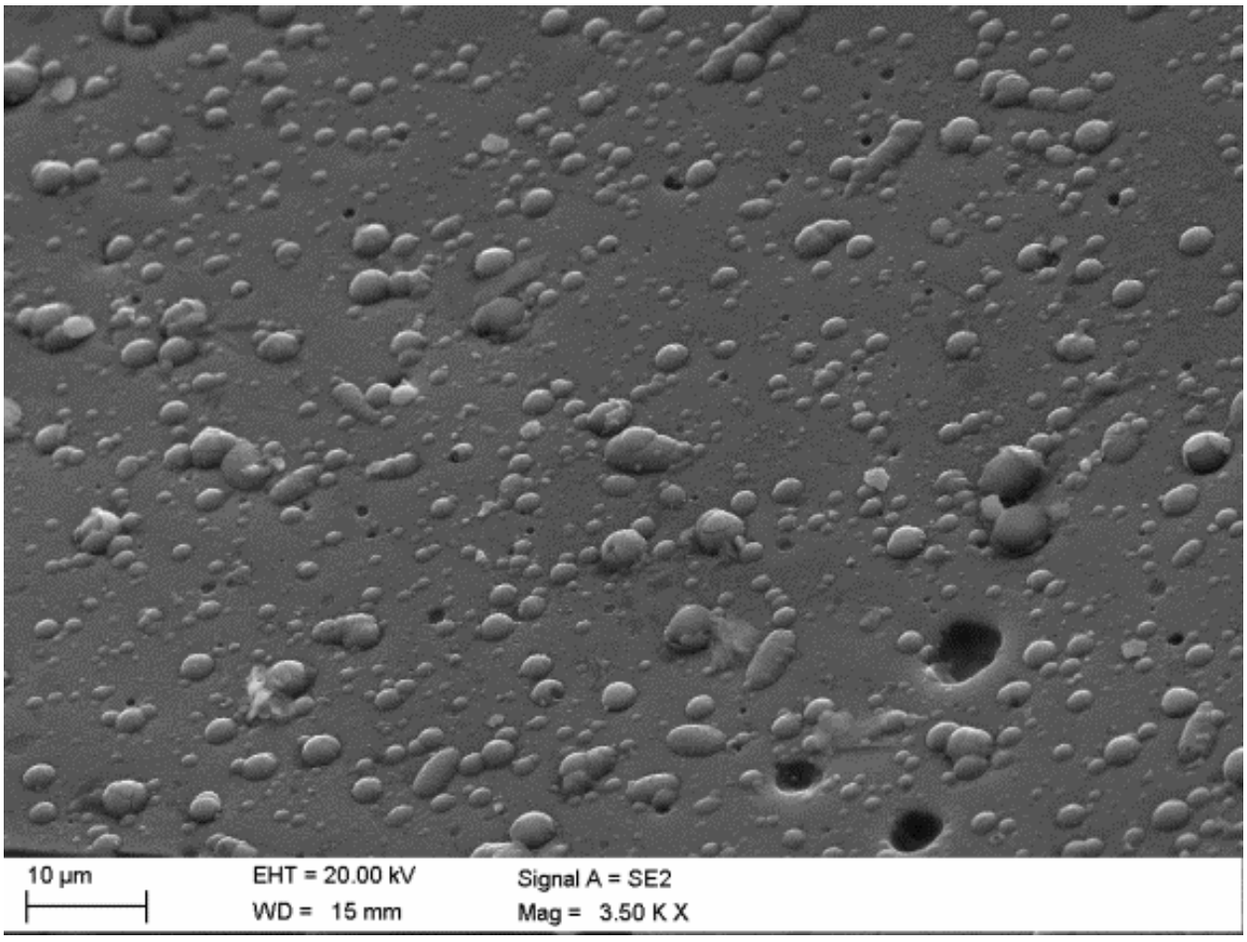

Figure 19. Surface topography of the Ti/TiCN/TiAlN coating deposited onto AZ61 substrate

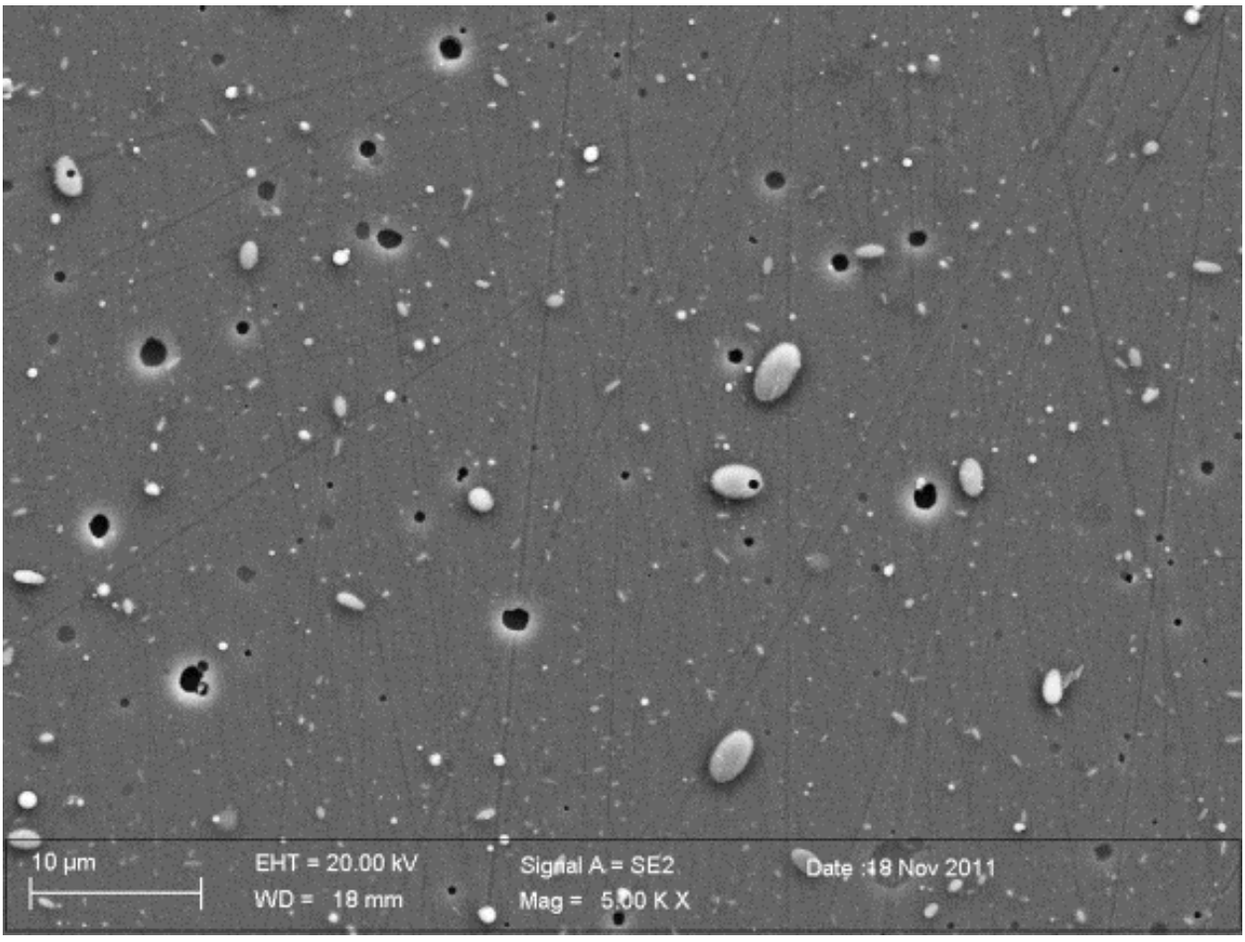

Figure 20. Surface topography of the Cr/CrN/CrN coating deposited onto AZ91 substrate

Based on the results obtained by the quantitative X-ray microanalysis using the energy dispersed X-ray EDS spectrometer it was confirmed the presence of Mg, Al, Zn, Ti, C as major alloying elements of the cast magnesium alloys as well the obtained coatings (Fig. 22, Table 5). Due to the fact, that the EDS analysis in case of measurement of so called light element concentrations, for which the energy <1 keV (C) has a relatively large measurement error because of strong absorption. For this reason the described values should be seen as estimated values only. But the measurement error in case of mass concentration measurement - in the range from 5 to 20 % - is about 2%.

Chemical element	The mass and atomic concentration of main elements, %	
	mass	atomic
	Analysis 1 (point 1)	
C	92.85	96.92
Mg	04.33	02.24
Al	00.52	00.24

Ti	02.29	00.60
Matrix	Correction	ZAF
	Analysis 2 (point 2)	
C	76.59	89.31
Zn	00.84	00.18
Mg	12.56	07.23
Al	01.55	00.81
Ti	08.46	02.47
Matrix	Correction	ZAF
	Analysis 2 (point 3)	
Zn	05.67	02.25
Mg	67.38	71.85
Al	26.95	25.90
Matrix	Correction	ZAF

Table 5. The results of quantitative chemical analysis from third 1, 2, 3 areas of coating Ti/DLC/DLC deposited onto substrate from AZ91 alloy marked in Fig. 22

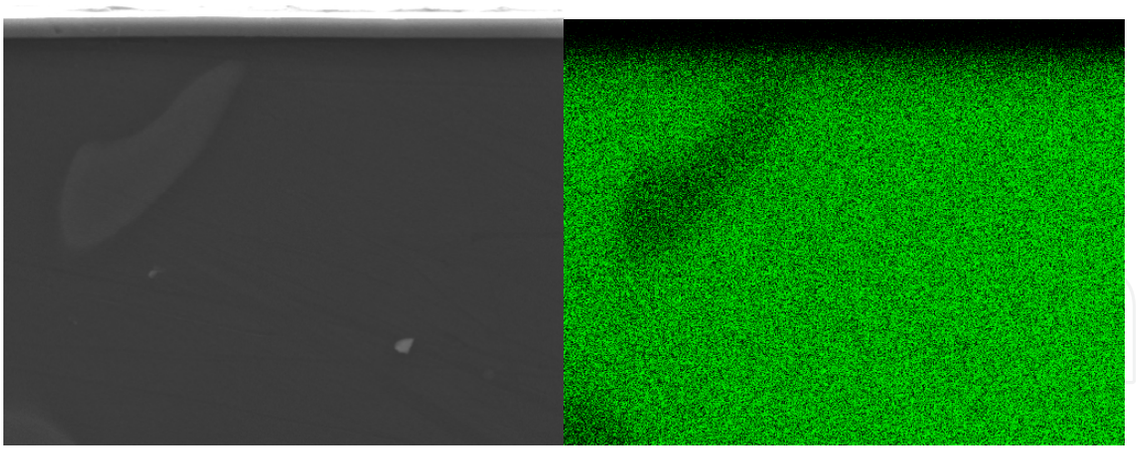

SE Mg

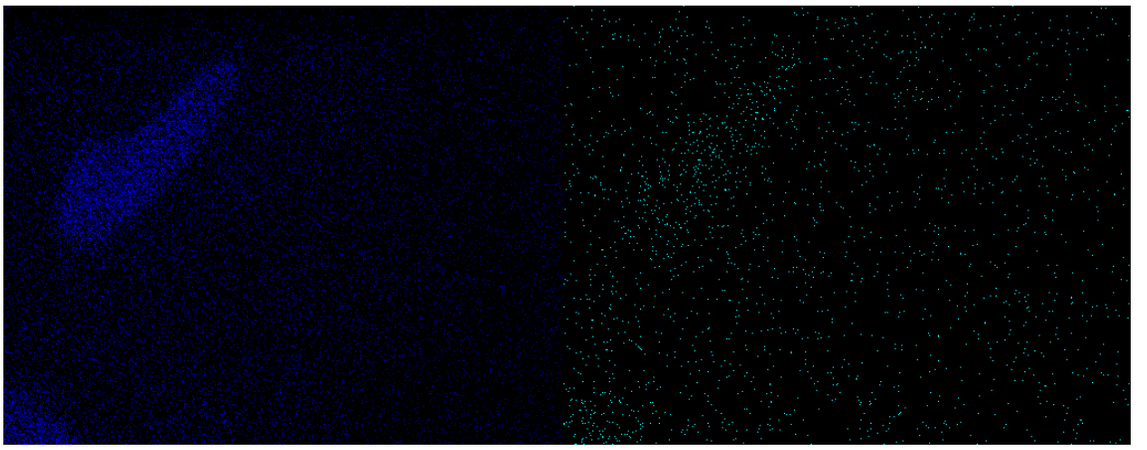

Al Zn

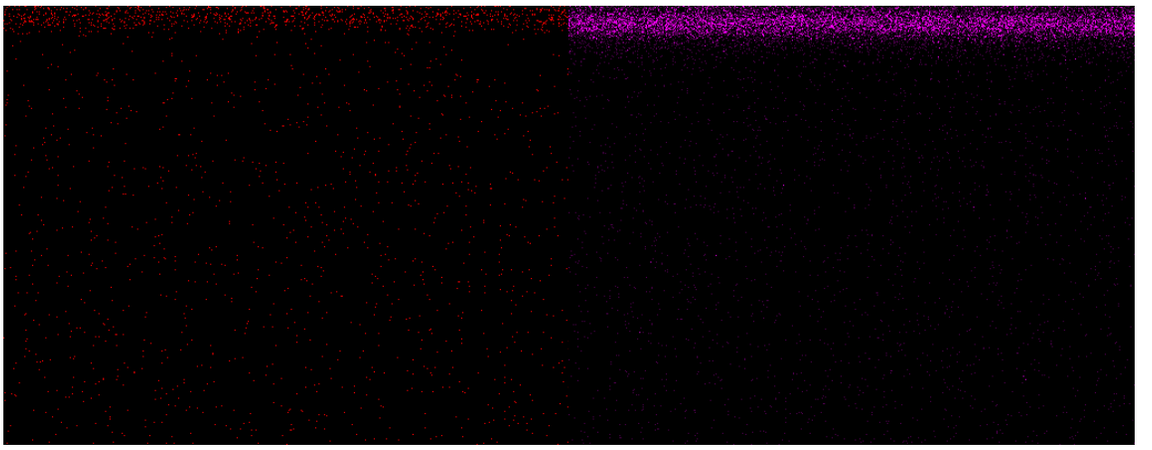

N Cr

Figure 21. The area analysis of chemical elements of the Cr/CrN/CrN coating and the magnesium (AZ61) substrate: image of the secondary electrons (A) and maps of elements' distribution

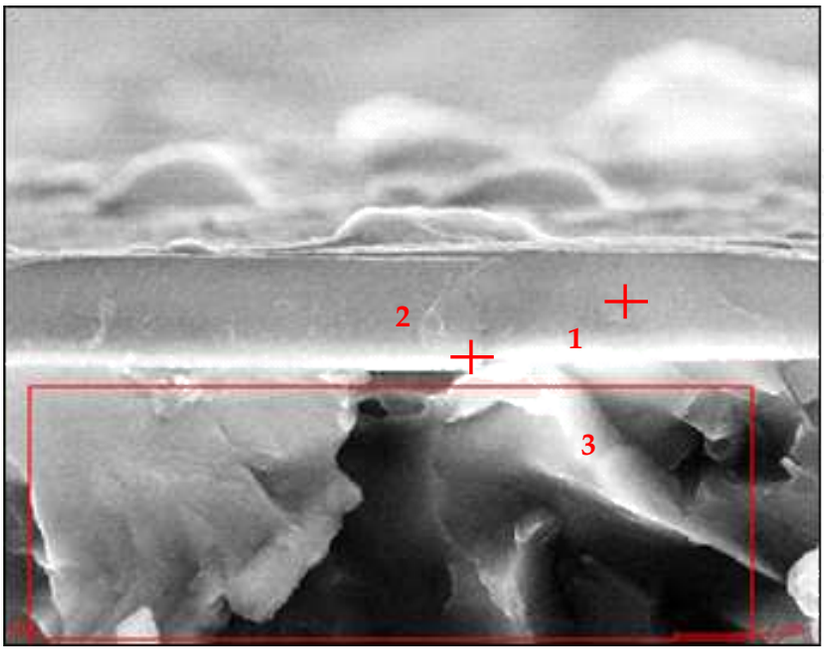

Figure 22. Cross-section SEM images of the Ti/DLC/DLC coating deposited onto the AZ91 substrate

Changes of coating component concentration and substrate material made in GDOS were presented in Figs. 23, 24. The tests carried out with the use of GDOS indicate the occurrence of a transition zone between the substrate material and the coating, which results in the improved adhesion between the coatings and the substrate. In the transition zone between the coatings and the substrate, the concentration of the elements of the substrate increases with simultaneous rapid decrease in concentration of elements contained in the coatings. The existence of the transition zone should be connected with high-energy ion action that caused mixing of the elements in the interface zone.

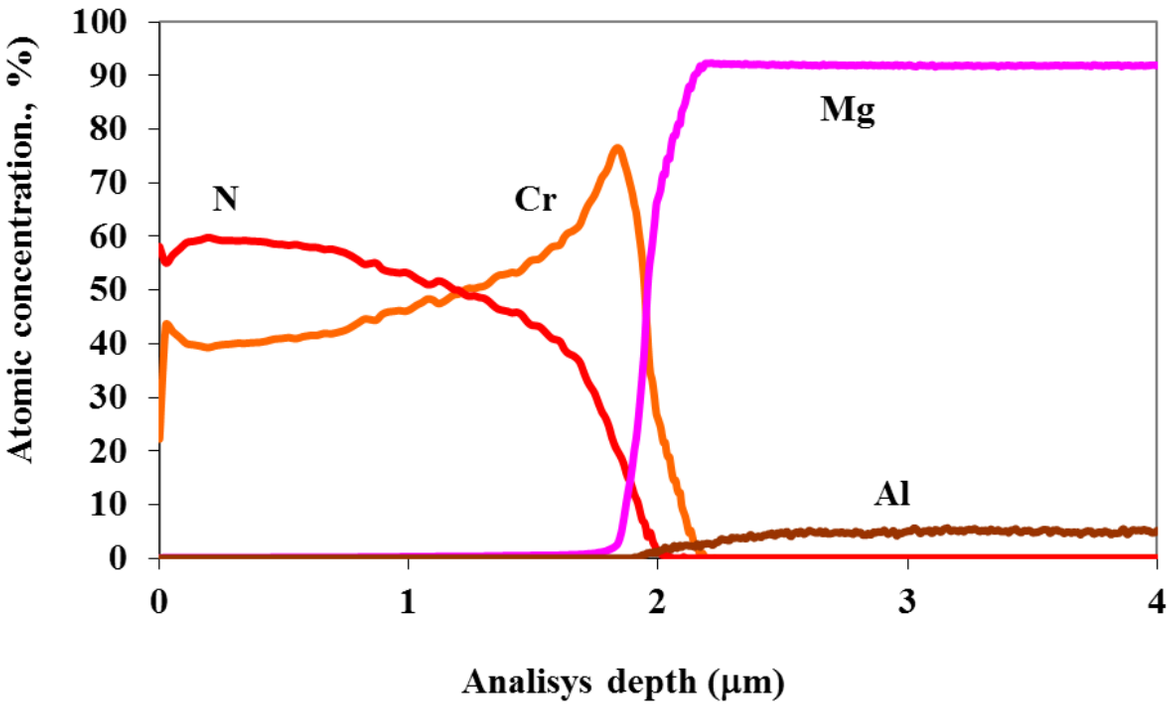

Figure 23. Changes of constituent concentration of the Cr/CrN/CrN and the AZ61 substrate materials

http://dx.doi.org/10.5772/48165

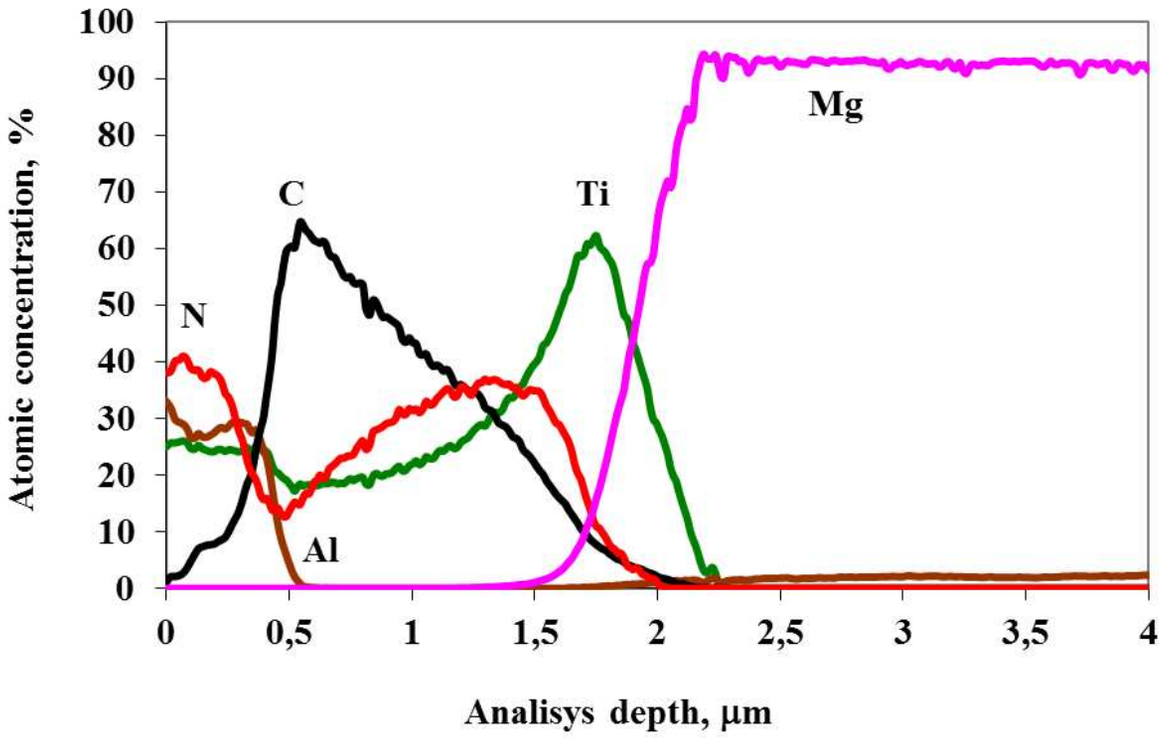

Figure 24. Changes of constituent concentration of the Ti/TiCN/TiAlN and the AZ61 substrate materials

On Figs. 25 a and b there are presented the X-ray diffractions of the investigated magnesium alloys in state after heat treatment. Using the of qualitative X-ray phase analysis methods it was confirmed, that in the investigated materials occurs the γ ($Mg_{17}Al_{12}$) phase as well the α-Mg phase which is the alloy matrix. A too small volume fraction of other phases present in the material does not allow it to perform an unambiguous identification of the obtained X-ray diffractions. Because of the overlapping reflections of the substrate and the coating material, as well the relatively small thickness of each layer, there were difficulties with identification of the phases. It was also confirmed the presence of reflexes coming from the phases present in the substrate, e.g. α and γ (Fig. 25 c,d). Very small volume fraction of other phases present in the substrate material does not allow it to perform an unambiguous identification of the recorded X-ray spectrum. The presence of substrate reflexes was confirmed on every achieved X-Ray diffraction collected from the coating, due to the thickness of the obtained coatings <3.5 µm, smaller than the X-ray penetration depth. Using the technique of fixed incidence angle (GIXRD method) there are collected only reflexes from the thin surface layers (Fig. 25 e,f).

The morphology of the deposited films, particulary DLC coating was characterized also by Raman spectroscopy. This spectroscopy method was used to determine the microstructure and chemical composition of the deposited DLC films. The shape of the achieving Raman spectrum is characteristic for carbon materials with a low level of structure order. The ob-

tained spectrum can be presented in form of two Gaussian curves, respectively for the Ram-

an shift values equal ca 1500 cm -1 (D band) and 1300 cm -1 (G band). The ratio of their

height can be presented as a ordering level of the carbon structure of the material analyzed.

The analyzed layer is composed of amorphous carbon - or more precisely- composed of

poorly structured carbon material, including small crystallites.

http://dx.doi.org/10.5772/48165

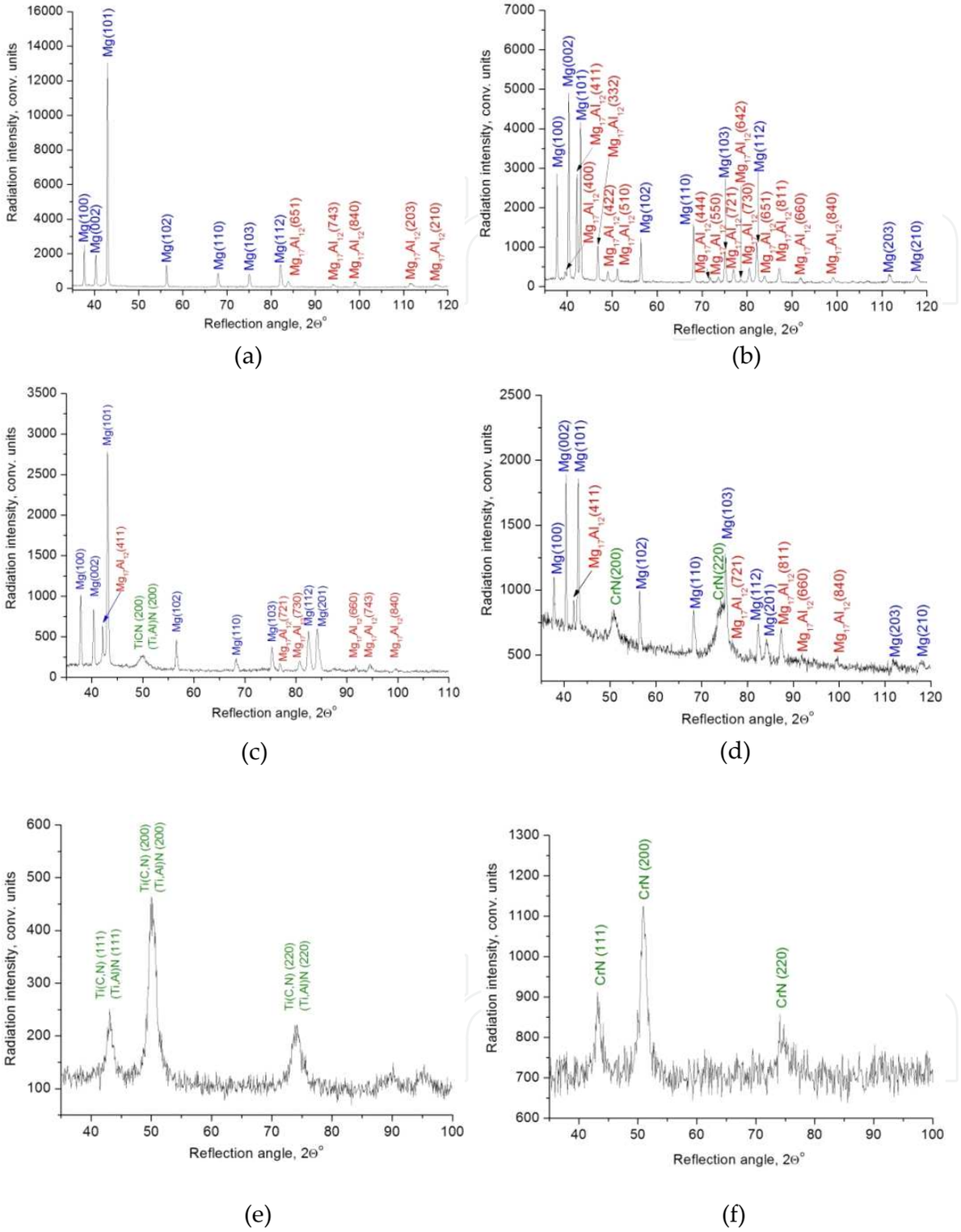

Figure 25. X-ray diffraction pattern of: a) AZ31 substrate, b) AZ121 substrate, c) Ti/TiCN/TiAlN coating deposited on the AZ91 magnesium alloys, d) Cr/CrN/CrN coating deposited on the AZ91 magnesium alloys obtained by Bragg-Brentano method, e) Ti/TiCN/TiAlN coating deposited on the AZ61 magnesium cast alloy obtained by GIXRD method (α=4°), f) Cr/CrN/CrN coating deposited on the AZ61 magnesium cast alloy obtained by GIXRD method (α=4°)

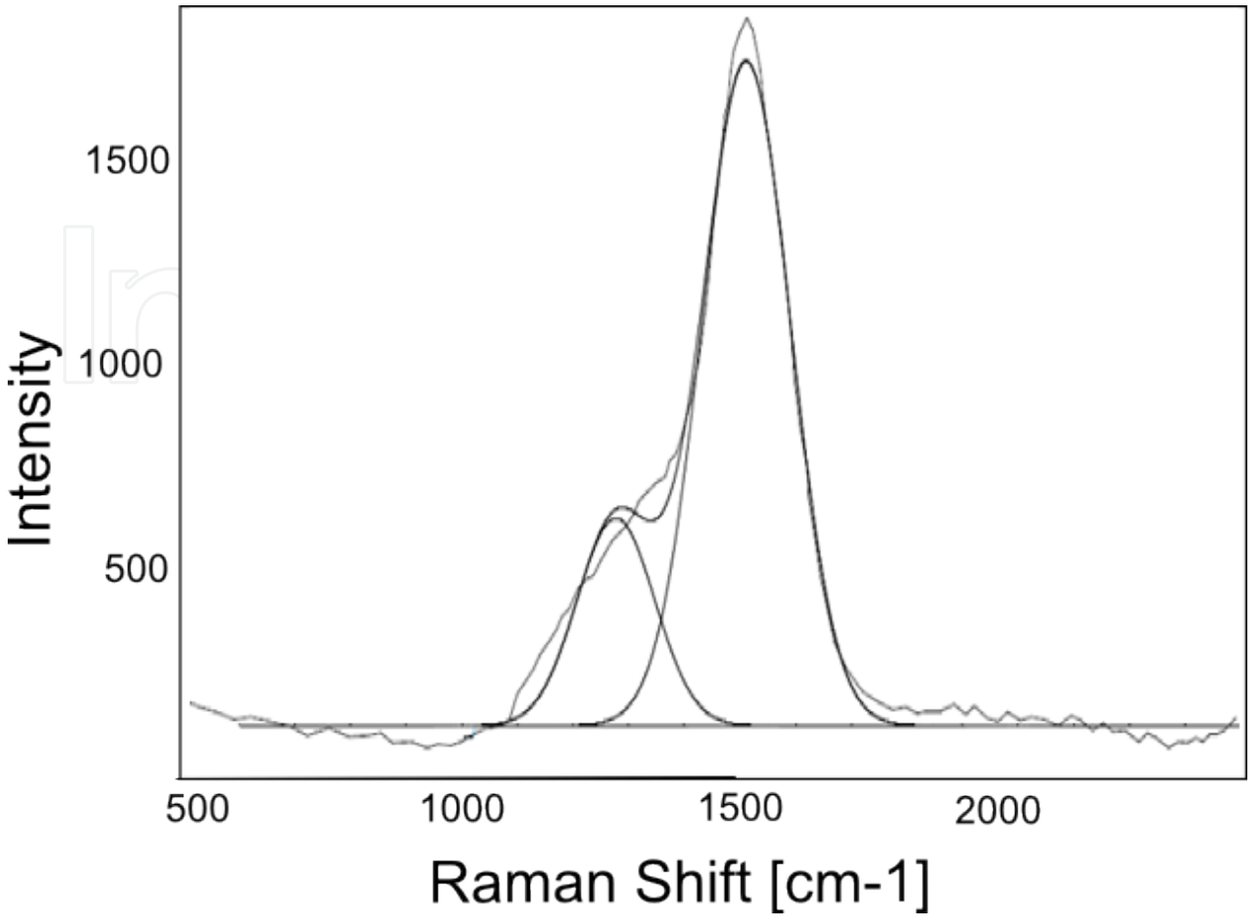

Figure 26. Raman spectra of the DLC films deposited on AZ91 magnesium alloys.

The highest value of surface roughness equal 0.3 mm was measured for the coating of the Ti/TiCN/TiAlN type which is likely caused by the occurrence of numerous microparticles in the shape of droplets in the structure (Table 6, Figure 13, 14, 19). The observed high homogeneity of the Cr/CrN/CrN surface coating is characterized by a smaller amount of crystallised droplets of liquid metal (Table 6, Figure 20), what responses to a smaller surface roughness within the range from 0.12 to 0.15 mm. The Ti/DLC/DLC coating has a surface roughness of ~ 0.25 mm. The performed investigations of the surface of the cast magnesium alloy, with coated layers confirm a lack of significant effect of the substrate type on the surface roughness (Table 6).

To determine the tribological properties of the investigated coating deposited on the magnesium alloys substrate, an abrasion test under dry slide friction conditions was carried out by the ball-on-disk method. Table 6 and Fig. 27 presents the friction coefficient and sliding distance results for each type of the investigated substrate. Under technically dry friction conditions, after the wearing-in period, the friction coefficient recorded for the associations tested is stabilized in the range 0.08-0.38 μm depending on the used substrate and coatings. All friction coefficient diagrams which were collected depending on the rotation rate or friction path length have similar characteristics and can be divided into two parts (Fig. 27). In the

http://dx.doi.org/10.5772/48165

first part, there occurs a sharp increase of the friction coefficient together with increasing friction path length. It was assumed, that this is a transient state of the friction process. The second part of the graph has already a stable state. Rapid changes of the friction coefficient value are caused by the occurrence of pollutants in form of sample counterface spalling products (balls are made from WC), which disturb the measurement of the friction coefficient. Comparing the friction coefficient results with the friction path length, it was found that the best wear resistance is characteristic for materials coated with DLC carbon. According to the applied load of 5 N, the average friction coefficients for the DLC coatings with the sliding rate of 0.05 m / s is in the range of 0.08-0.15 mm, which is ten times lower compared to the friction coefficient values of other examined coatings. However, the results of the friction path length for the DLC coatings were at a level exceeding even 70 times the results of the friction path length achieved for the Cr/CrN/CrN coatings. This is characteristic for DLC coatings, because they are composed of poorly ordered graphite, which is probably formed by a friction-assisted phase transformation of the surface layer of the DLC matrix and acts as a lubricant at the surface [17]. Accordingly, the high hardness of DLC together with this transfer layer is responsible for the low friction coefficient of the DLC film in comparison with magnesium alloys coated other investigated coatings. At high sliding speed, the transfer layer is more easily formed due to the accumulation of heat, resulting in a lower friction coefficient.

AZ121			
Coatings	**Roughness [µm]**	**Friction coefficient, [µm]**	**Sliding disance, [m]**
Cr/CrN/CrN	0.13	0.24-0.27	8
Ti/TiCN/TiAlN	0.28	0.19-0.22	59.4
Ti/DLC/DLC	0.24	0.09-0.16	550
AZ91			
Coatings	**Roughness [µm]**	**Friction coefficient, [µm]**	**Sliding disance, [m]**
Cr/CrN/CrN	0.12	0.25-0.38	7.8
Ti/TiCN/TiAlN	0.27	0.18-0.25	57.6
Ti/DLC/DLC	0.25	0.1-0.17	540
AZ61			
Coatings	**Roughness [µm]**	**Friction coefficient, [µm]**	**Sliding disance, [m]**
Cr/CrN/CrN	0.15	0.22-0.28	22
Ti/TiCN/TiAlN	0.30	0.17-0.22	77.7
Ti/DLC/DLC	0.25	0.09-0.19	630

AZ31			
Coatings	**Roughness [µm]**	**Friction coefficient, [µm]**	**Sliding disance, [m]**
Cr/CrN/CrN	0.12	0.2-0.29	13
Ti/TiCN/TiAlN	0.28	0.15-0.22	66
Ti/DLC/DLC	0.26	0.08-0.15	605

Table 6. The characteristics of the tested coatings

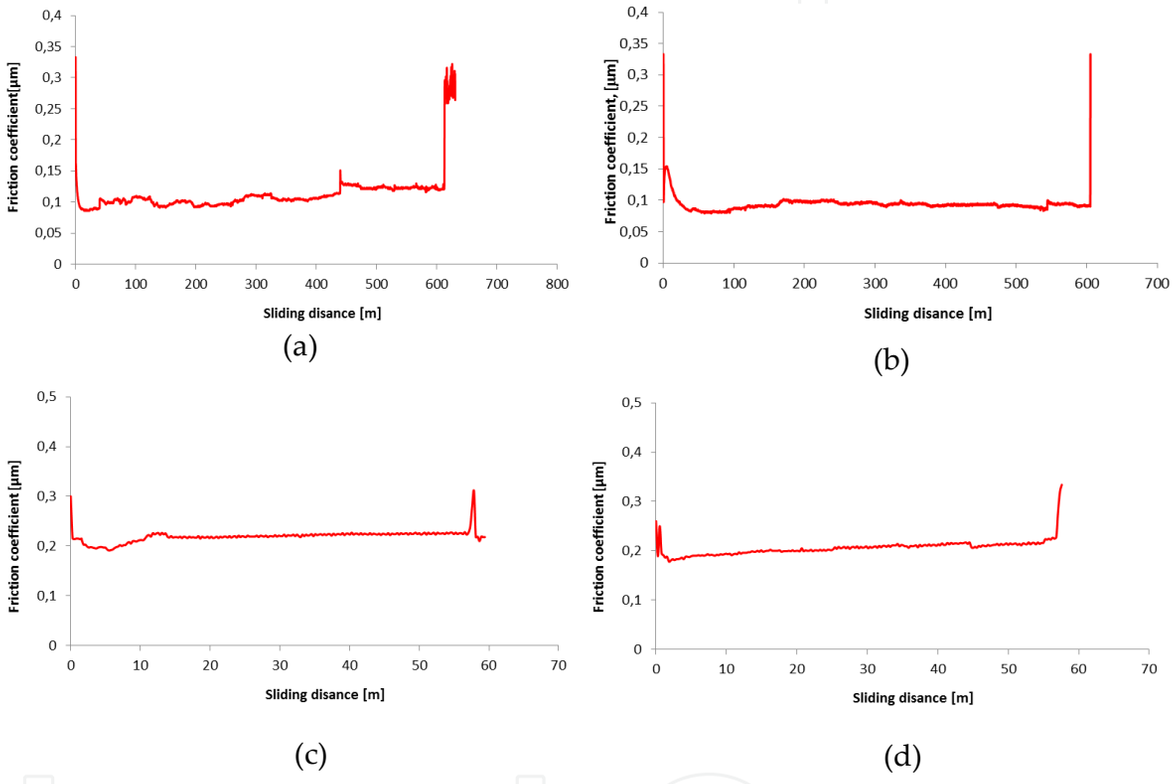

Figure 27. Dependence of friction coefficient on sliding distance during the wear test for: a) Ti/DLC/DLC coating deposited on the AZ61, b) Ti/DLC/DLC coating deposited on the AZ31, c) Ti/TiCN/TiAlN coating deposited on the AZ121, d) Ti/TiCN/TiAlN coating deposited on the AZ91

7. Summary

Due to the character of the investigated material (magnesium alloys) and its relatively low melting point, the whole technological PVD and PACVD processes were performed at temperatures up to 150 °C for Cr/CrN/CrN coatings and Ti/TiCN/TiAlN coatings, and up to 180° C for Ti/DLC/DLC coatings. Results of diffraction method investigations achieved by the high resolution transmission electron microscope allow to identify the TiAlN, CrN,

graphit phase occurred in the surface layer. It was found out, as a result of the microstructure investigations on scanning electron microscope, that there are no pores or cracks in the produced coating and no defects and failures occurring spontaneously in this single layer are of significant importance for the properties of the whole layer. Coating thickness was measured using a scanning electron microscope. The thickness of the Ti/TiCN/TiAlN layer is in the range up to 3.3 μm, Cr/CrN/CrN layer is in the range up to 1.9 μm, and Ti/DLC/DLC layer is in the range up to 2.5 microns. The tests carried out with the use of GDOS indicate the occurrence of a transition zone between the substrate material and the coating, which results in the improved adhesion between the coatings and the substrate. Using the technique of fixed incidence angle (GIXRD method) there are collected only reflexes from the thin surface layers. The highest wear resistance was obtained for the of Ti/DLC/DLC coating.

Acknowledgement

Research was financed partially within the framework of the Polish State Committee for Scientific Research Project No. 4688/T02/2009/37 headed by Dr Tomasz Tański

Author details

Tomasz Tański

Faculty of Mechanical Engineering, Silesian University of Technology, Gliwice,, Poland

References

[1] Horst EF, Mordike BL(2006). Magnesium Technology. Metallurgy, Design Data, Application, Springer-Verlag, Berlin Heidelberg, 2006. 707 p.

[2] Tański, T., Dobrzański, L. A., & Labisz, K. (2010). Investigations of microstructure and dislocations of cast magnesium alloys. Journal of Achievements in Materials and Manufacturing Engineering. 42/1-2: 94-101.

[3] Easton, M., Beer, A., Barnett, M., Davies, C., Dunlop, G., Durandet, Y., Blacket, S., Hilditch, T., & Beggs, P. (2008). Magnesium Alloy Applications in Automotive Structures. Journal Minerals, Metals and Materials Society. , 60, 57-62.

[4] Mehta DS, Masood SH, Song WQ(2004). Investigation of wear properties of magnesium and aluminium alloys for automotive applications. Journal of Materials Processing Technology. 155-156:1526-1531.

[5] Dobrzański, L. A., Tański, T., & Čížek, L. (2006). Influence of Al addition on microstructure of die casting magnesium alloys. Journal of Achievements in Materials and Manufacturing Engineering , 19, 49-55.

[6] Dobrzański, L. A., Tański, T., & Čížek, L. (2007). Heat treatment impact on the structure of die-cast magnesium alloys. Journal of Achievements in Materials and Manufacturing Engineering. , 20, 431-434.

[7] Tański, T., Dobrzański, L. A., & Čížek, L. (2007). Influence of heat treatment on structure and properties of the cast magnesium alloys. Journal of Advanced Materials Research. 15-17: 491-496.

[8] Dobrzański, L. A., & Tański, T. (2009). Influence of aluminium content on behaviour of magnesium cast alloys in bentonite sand mould. Solid State Phenomena. 147-149: 764-769.

[9] Dobrzański, L. A., Tański, T., Malara, Sz., Król, M., & Domagała-Dubiel, J. (2011). Contemporary forming methods of the structure and properties of cast magnesium alloys. In Czerwinski F, editor. Magnesium Alloys- Design, Processing and Properties. Rijeka: InTech. , 321-350.

[10] Tański, T., & Labisz, K. (2012). Electron microscope investigation of PVD coated aluminium alloy surface layer. Solid State Phenomena , 186, 192-197.

[11] Tański, T., & Lukaszkowicz, K. (2011). Structure and mechanical properties of hybrid-layers coated applying the PVD method onto magnesium and aluminium alloys substrate. Materials Engineering. , 4, 772-775.

[12] Lukaszkowicz, K., Czyżniewski, A., Kwaśny, W., & Pancielejko, M. (2011). Structure and mechanical properties of PVD coatings deposited onto the X40CrMoVhot work tool steel substrate. Vacuum. 2011 in print., 5-1.

[13] Hollstein, F., Wiedemann, R., & Scholz, J. (2003). Characteristics of PVD-coatings on AZ31HP magnesium alloys. Surface and Coatings Technology. , 162, 261-268.

[14] Veprek, S., & Veprek-Heijman, M. J. G. (2008). Industrial applications of superhard nanocomposite coatings. Surface & Coatings Technology. , 202, 5063-5073.

[15] Alvarez, J., Melo, D., Salas, O., Reichelt, R., Oseguera, J., & Lopez, V. (2009). Role of Al oxide PVD coatings in the protection against metal dusting. Surface & Coatings Technology. , 204, 779-83.

[16] Dobrzański, L. A., & Staszuk, M. (2010). PVD and CVD gradient coatings on sintered carbides and sialon tool ceramics. Journal of Achievements in Materials and Manufacturing Engineering. 43/, 2, 552-576.

[17] Zou, Y. S., Wu, Y. F., Yang, H., Cang, K., Song, G. H., Li, Z. X., & Zhou, K. (2011). Applied Surface Science. , 258, 1624-1629.